

# Normal modes for $N$ identical particles: A study of the evolution of collective behavior from few-body to many-body

D. K. Watson

University of Oklahoma

Homer L. Dodge Department of Physics and Astronomy

Norman, OK 73019

(Dated: February 28, 2022)

Normal mode dynamics are ubiquitous in nature underlying the motions of diverse interacting systems from the behavior of rotating stars to the vibration of crystal structures. These behaviors are composed of simple collective motions of the  $N$  interacting particles which move with the same frequency and phase, thus encapsulating many-body effects into simple dynamic motions. In some regimes these collective motions are coupled by higher order effects and exhibit complex behavior, while in regimes such as the unitary regime for ultracold Fermi gases, a single collective mode can dominate, leading to quite simple behavior as seen in superfluidity. In this study, I investigate the evolution of collective motion as a function of  $N$  for five types of normal modes obtained from an  $L = 0$  group theoretic solution of a general Hamiltonian for confined, identical particles. I show using simple analytic forms for the  $N$ -body normal modes that the collective behavior of few-body systems, which have the well known motions of molecular equivalents such as ammonia and methane, evolves smoothly as  $N$  increases to the collective motions expected for large  $N$  ensembles (breathing, center of mass, particle-hole radial and angular excitations and phonon). Furthermore, the transition from few-body behavior (symmetric stretch, symmetric bend, antisymmetric stretch, antisymmetric bend and the opening and closing of alternative interparticle angles) to large  $N$  behavior occurs at quite low values of  $N$ . By  $N = 10$ , the behavior of these normal modes has clearly become the expected large  $N$  behavior that describes ensembles with  $10^{23}$  particles or more. I extend this investigation to a Hamiltonian known to support collective behavior, the Hamiltonian for Fermi gases in the unitary regime. I analyze both the evolution of the coefficients that mix the radial and angular symmetry coordinates in the expressions for the normal modes as well as the evolution of the normal mode frequencies as a function of  $N$ . Both quantities depend on interparticle interactions. This analysis reveals two phenomena that could contribute to the viability of collective behavior. First the coefficients that mix radial and angular coordinates in the normal modes go to zero or unity, i.e. no mixing, as  $N$  becomes large resulting in solutions that do not depend on the details of the interparticle potential as expected for this unitary regime, and that manifest the symmetry of an underlying approximate Hamiltonian. Second, the five normal mode frequencies which all start out close to the trap frequency for low values of  $N$  ( $N < 10$ ) separate rapidly as  $N$  increases, creating large gaps between the normal modes that can, in principle, offer stability to collective behavior if mechanisms to prevent the transfer of energy to other modes exist (such as low temperature) or can be constructed. With the recent success using normal modes to describe the emergence of collective behavior in the form of superfluidity in ultracold Fermi gases in the unitary regime, understanding the character of these normal modes and the evolution of their behavior as a function of  $N$  has become of some interest due to the possibility of offering insight into the dynamics of regimes supporting collective behavior. In this study, I investigate both the macroscopic behavior associated with these  $N$ -body normal modes, as well as the microscopic motions underlying this behavior, and study the evolution of their collective behavior as a function of  $N$ .

## I. INTRODUCTION

Normal modes occur in every part of the universe and at all scales from nuclear physics to cosmology. They have been used to model the behavior of a variety of physical systems including atmospheres[1], seismic activity of the earth[2], global ocean behavior[3], vibrations of crystals[4], molecules[5], and nuclei[6], functional motions of proteins, viruses and enzymes[7], the oscillation of rotating stars[8], gravitational wave response[9], black hole oscillations[10], liquids[11], ultracold trapped gases[12], and cold trapped ions for quantum information processing[13]. Reflecting the ubiquitous appearance of small vibrations in nature, normal modes couple the com-

plex motion of individual interacting particles into simple collective motions in which the particles move in sync with the same frequency and phase. Systems in equilibrium experiencing small perturbations tend to return to equilibrium if restorative forces are present. These restorative forces can often be approximated by effective harmonic terms that couple the  $N$  particles in these systems resulting in dynamics that can be transformed to that of  $N$  uncoupled oscillators whose collective coordinates define the normal modes. The power of normal modes lies in their ability to describe the complex motion of  $N$  interacting particles in terms of collective coordinates whose character and frequencies reflect the inter-particle correlations of the system, thus incorporating many-body effects into simple dynamic motions.

Higher order effects can be expanded in this physically intuitive basis of normal modes. If higher order (e.g. anharmonic) effects are small, these collective motions are eigenfunctions of an approximate Hamiltonian acquiring some measure of stability as a function of time; thus, a system in a single normal mode will have a tendency to remain in that mode until perturbed. Normal modes manifest the symmetry of this underlying approximate Hamiltonian with the possibility of offering analytic solutions to a many-body problem and a clear physical picture of the dynamics.

Confined quantum systems in the laboratory with  $N$  identical interacting particles have been shown to exhibit collective behaviors thought to arise from general and powerful principles of organization[14–18]. In a recent paper, collective behavior in the form of  $N$ -body normal modes successfully described the thermodynamic behavior associated with the superfluidity of an ultracold gas of fermions in the unitary regime[19]. Two normal modes, selected by the Pauli principle, were found to play a role in creating and stabilizing the superfluid behavior at low temperatures, a phonon mode at ultralow temperatures and a single particle radial excitation mode, i.e. a particle-hole excitation, as the temperature increases. This radial excitation has a much higher frequency and creates a gap that stabilizes the superfluid behavior. The two normal modes were found to describe the thermodynamic behavior of this gas quite well compared to experimental data.

These normal modes are the perturbation solutions at first order in inverse dimensionality of a first principle many-body formalism called symmetry invariant perturbation theory (SPT). This formalism uses a group theoretic approach for the solution of a fully interacting, many-body, three-dimensional Hamiltonian with an arbitrary interaction potential as well as a confining potential[20, 21]. Using the symmetry of the symmetric group which can be accessed at large dimension[22], this approach has successfully rearranged the many-body work needed at each order in the perturbation series so that an exact solution can, in principle, be obtained order-by-order using group theory and graphical techniques, i.e. non-numerically[25]. Specifically, the numerical work has been rearranged into analytic building blocks that allow a formulation that does not scale with  $N$ [21, 23–26]. Group theory is used to partition the  $N$  scaling problem away from the interaction dynamics, allowing the  $N$  scaling to be treated as a separate mathematical problem (cf. the Wigner-Eckart theorem). The exponential scaling is shifted from a dependence on the number of particles,  $N$ , to a dependence on the order of the perturbation expansion[26]. This allows one to obtain exact first-order results that contain beyond-mean-field effects for all values of  $N$  from a single calculation, but going to higher order is now exponentially difficult. The analytic building blocks have been calculated and stored to minimize the work needed for new calculations[27]. Since the perturbation does not involve the strength of

the interaction, strongly interacting systems can be studied.

Initially applied to systems of cold bosons, my group has previously derived beyond-mean-field energies[22, 28], frequencies[28], normal mode coordinates[20], wave functions[20] and density profiles[29] for general isotropic, interacting confined quantum systems of identical bosons. Recently I have extended this formalism to systems of fermions[19, 30–32]. I avoid the numerically demanding construction of explicitly antisymmetrized wave functions by applying the Pauli principle at first order “on paper” through the assignment of appropriate normal mode quanta[30, 31]. I have determined ground[30] and excited state[19] beyond-mean-field energies and their degeneracies allowing the construction of a partition function[32].

Analytic expressions for these normal modes have been obtained in a previous paper, Ref. [20]. In Sections 5 and 6 of Ref. [20], we discussed the symmetry of the  $N$ -body quantum-confinement problem at large dimension which greatly simplifies the problem, making possible, in principle, an exact solution of this  $N$ -body problem, with  $N(N - 1)/2$  interparticle interactions order-by-order. In Section 7 we exploited this symmetry, deriving symmetry coordinates used in the determination of the normal modes of the system. We introduced a particular approach to derive a suitable basis of symmetry coordinates that builds up the complexity slowly and systematically. This is illustrated in detail for each of the five types of symmetry coordinates that transform under the five different irreducible representations for a system of  $N$  identical particles. In Section 8 we applied this general theory to derive in detail analytic expressions for the normal-mode coordinates.

These functions serve as a natural basis for the determination of higher order terms in the perturbation series, and they offer the possibility of a clear physical picture of the dynamics if higher order terms are small. One major advantage of this approach is that  $N$  appears as a parameter in the analytical expressions for the normal modes, as well as the energy spectrum, so the behavior of these modes can be easily studied as a function of  $N$ .

The quantum wave function yields important information about the dynamics of a system beyond that obtainable from the energy spectrum. Although explicit antisymmetrized wave functions are not currently obtained in this SPT formalism, the normal mode solutions at first order constitute a complete basis. Thus the character of the wave function may be revealed if a single normal mode is dominant since the normal modes have clear, macroscopic motions.

In this paper, I expand on our earlier discussion of these analytic normal modes, examining in detail the motion of individual particles as they contribute to the five types of normal modes for an  $N$ -body system of identical particles under quantum confinement. In particular, I study the evolution of collective behavior as a function of  $N$  from few-body systems to many-body systems,

first making general observations and then choosing as a specific case the Hamiltonian for a confined system of fermions in the unitary regime which is known to support collective behavior. Finally in the Appendices, I present additional details of the derivation of these normal modes.

## II. REVIEW OF THE N-BODY NORMAL MODE DERIVATION

In this Section, I briefly review the derivation of the normal modes that was presented in more detail in Ref. [20] as solutions to the SPT first order perturbation equation.

### A. D-dimensional N-body Schrödinger Equation

The  $D$ -dimensional Schrödinger equation in Cartesian coordinates for a system of  $N$  particles interacting via a two-body interaction potential  $g_{ij}$ , and confined by a spherically symmetric potential  $V_{\text{conf}}$  is

$$H\Psi = \left[ \sum_{i=1}^N h_i + \sum_{i=1}^{N-1} \sum_{j=i+1}^N g_{ij} \right] \Psi = E\Psi, \quad (1)$$

$$\begin{aligned} h_i &= -\frac{\hbar^2}{2m_i} \sum_{\nu=1}^D \frac{\partial^2}{\partial x_{i\nu}^2} + V_{\text{conf}} \left( \sqrt{\sum_{\nu=1}^D x_{i\nu}^2} \right), \\ g_{ij} &= V_{\text{int}} \left( \sqrt{\sum_{\nu=1}^D (x_{i\nu} - x_{j\nu})^2} \right), \end{aligned} \quad (2)$$

where  $h_i$  is the single-particle Hamiltonian and  $x_{i\nu}$  is the  $\nu^{\text{th}}$  Cartesian component of the  $i^{\text{th}}$  particle. Transforming the Schrödinger equation from Cartesian to the internal coordinates is accomplished using:

$$\begin{aligned} r_i &= \sqrt{\sum_{\nu=1}^D x_{i\nu}^2}, \quad (1 \leq i \leq N), \\ \gamma_{ij} &= \cos(\theta_{ij}) = \left( \sum_{\nu=1}^D x_{i\nu} x_{j\nu} \right) / r_i r_j, \end{aligned} \quad (3)$$

( $1 \leq i < j \leq N$ ), which are the  $D$ -dimensional scalar radii  $r_i$  of the  $N$  particles from the center of the confining potential and the cosines  $\gamma_{ij}$  of the  $N(N-1)/2$  angles between the radial vectors.

A similarity transformation removes the first-order derivatives, while the second derivative terms drop out in the  $D \rightarrow \infty$  limit, yielding a static zeroth-order problem. First order corrections result in simple harmonic normal-mode oscillations about the infinite-dimensional structure.

The Schrödinger equation becomes[33],  $(T + V)\Phi = E\Phi$  where:

$$T = \hbar^2 \sum_{i=1}^N \left[ -\frac{1}{2m_i} \frac{\partial^2}{\partial r_i^2} - \frac{1}{2m_i r_i^2} \sum_{j \neq i} \sum_{k \neq i} \frac{\partial}{\partial \gamma_{ij}} (\gamma_{jk} - \gamma_{ij} \gamma_{ik}) \frac{\partial}{\partial \gamma_{ik}} + \frac{N(N-2) + (D-N-1)^2 \left( \frac{\Gamma^{(i)}}{\Gamma} \right)}{8m_i r_i^2} \right] \quad (4)$$

$$V = \sum_{i=1}^N V_{\text{conf}}(r_i) + \sum_{i=1}^{N-1} \sum_{j=i+1}^N V_{\text{int}}(r_{ij}), \quad (5)$$

$\Gamma$  is the Gramian determinant of the matrix with elements  $\gamma_{ij}$  (see Appendix D in Ref [22]), and  $\Gamma^{(i)}$  is the determinant of the  $i^{\text{th}}$  principal minor where the row and column of the  $i^{\text{th}}$  particle have been deleted. The quantity  $r_{ij} = \sqrt{r_i^2 + r_j^2 - 2r_i r_j \gamma_{ij}}$  is the interparticle separation. From Eq. (4), it is clear that all first-order derivatives have been eliminated from the Hamiltonian.

### B. Infinite-D analysis: Zeroth-order energy

Dimensionally scaled variables are defined:  $\bar{r}_i = r_i / \kappa(D)$ ,  $\bar{E} = \kappa(D)E$  and  $\bar{H} = \kappa(D)H$ , where  $\kappa(D)$  is a scale factor that regularizes the large-dimension limit of the Schrödinger equation. The exact form of  $\kappa(D)$  is not fixed, but can be chosen to yield scaling results that are as simple as possible while satisfying  $\kappa(D) \sim D^2$ . Examples of  $\kappa(D)$  for different systems are given after Eq. (10) of Ref. [29].

The factor of  $\kappa(D)$  plays the role of an effective mass that increases with  $D$ , suppressing the derivative terms but leaving a centrifugal-like term in an effective poten-

tial,

$$\begin{aligned} \bar{V}_{\text{eff}}(\bar{r}, \gamma; \delta = 0) &= \sum_{i=1}^N \left( \frac{\hbar^2}{8m_i \bar{r}_i^2} \frac{\Gamma^{(i)}}{\Gamma} + \bar{V}_{\text{conf}}(\bar{r}, \gamma; \delta = 0) \right) \\ &+ \sum_{i=1}^{N-1} \sum_{j=i+1}^N \bar{V}_{\text{int}}(\bar{r}, \gamma; \delta = 0), \end{aligned} \quad (6)$$

where  $\delta = 1/D$ , and the particles become frozen at large  $D$ . We assume all radii and angle cosines of the particles are equal when  $D \rightarrow \infty$ , i.e.  $\bar{r}_i = \bar{r}_\infty$  ( $1 \leq i \leq N$ ) and  $\gamma_{ij} = \bar{\gamma}_\infty$  ( $1 \leq i < j \leq N$ ) where  $\bar{r}_\infty$  and  $\bar{\gamma}_\infty$  satisfy:

$$\left[ \frac{\partial \bar{V}_{\text{eff}}(\bar{r}, \gamma; \delta)}{\partial \bar{r}_i} \right]_{\delta=0} = 0, \quad \left[ \frac{\partial \bar{V}_{\text{eff}}(\bar{r}, \gamma; \delta)}{\partial \gamma_{ij}} \right]_{\delta=0} = 0, \quad (7)$$

resulting in a maximally symmetric structure. In scaled units the zeroth-order ( $D \rightarrow \infty$ ) approximation for the energy is:  $\bar{E}_\infty = \bar{V}_{\text{eff}}(\bar{r}_\infty)$ , while the centrifugal-like term in  $\bar{V}_{\text{eff}}$ , which is nonzero even for the ground state, is a zero-point energy contribution from the minimum uncertainty principle[34].

### C. The 1/D first-order energy correction

At zeroth-order, the particles can be viewed as frozen in a maximally symmetric, high- $D$  configuration. Solving Eqs. (7) for  $\bar{r}_\infty$  and  $\bar{\gamma}_\infty$  yields the infinite- $D$  structure and zeroth-order energy providing the starting point for the  $1/D$  expansion. In order to determine the  $1/D$  quantum correction to the energy for large but finite values of  $D$ , we expand about the minimum of the  $D \rightarrow \infty$  effective potential. A position vector of the  $N(N+1)/2$  internal coordinates is defined as:

$$\begin{aligned} \bar{\mathbf{y}} &= \begin{pmatrix} \bar{\mathbf{r}} \\ \bar{\boldsymbol{\gamma}} \end{pmatrix}, \quad \text{where} \quad \boldsymbol{\gamma} = \begin{pmatrix} \gamma_{12} \\ \gamma_{13} \\ \gamma_{23} \\ \gamma_{14} \\ \gamma_{24} \\ \gamma_{34} \\ \gamma_{15} \\ \gamma_{25} \\ \vdots \\ \gamma_{N-2,N} \\ \gamma_{N-1,N} \end{pmatrix}, \quad (8) \\ \text{and} \quad \bar{\mathbf{r}} &= \begin{pmatrix} \bar{r}_1 \\ \bar{r}_2 \\ \vdots \\ \bar{r}_N \end{pmatrix}. \end{aligned}$$

The following substitutions are made for all radii and angle cosines:  $\bar{r}_i = \bar{r}_\infty + \delta^{1/2} \bar{r}'_i$  and  $\gamma_{ij} = \bar{\gamma}_\infty + \delta^{1/2} \bar{\gamma}'_{ij}$  and a power series is obtained in  $\delta^{1/2}$  for the effective potential about the  $D \rightarrow \infty$  symmetric minimum:  $\left[ \frac{\partial \bar{V}_{\text{eff}}}{\partial \bar{y}_\mu} \right]_{\delta^{1/2}=0} = 0$ . Defining a displacement vector consisting of the internal displacement coordinates:

$$\begin{aligned} \bar{\mathbf{y}}' &= \begin{pmatrix} \bar{\mathbf{r}}' \\ \bar{\boldsymbol{\gamma}}' \end{pmatrix}, \quad \text{where} \quad \bar{\boldsymbol{\gamma}}' = \begin{pmatrix} \bar{\gamma}'_{12} \\ \bar{\gamma}'_{13} \\ \bar{\gamma}'_{23} \\ \bar{\gamma}'_{14} \\ \bar{\gamma}'_{24} \\ \bar{\gamma}'_{34} \\ \bar{\gamma}'_{15} \\ \bar{\gamma}'_{25} \\ \vdots \\ \bar{\gamma}'_{N-2,N} \\ \bar{\gamma}'_{N-1,N} \end{pmatrix}, \quad (9) \\ \text{and} \quad \bar{\mathbf{r}}' &= \begin{pmatrix} \bar{r}'_1 \\ \bar{r}'_2 \\ \vdots \\ \bar{r}'_N \end{pmatrix}, \end{aligned}$$

the expression for  $\bar{V}_{\text{eff}}$  becomes:

$$\begin{aligned} \bar{V}_{\text{eff}}(\bar{\mathbf{y}}'; \delta) &= [\bar{V}_{\text{eff}}]_{\delta^{1/2}=0} \\ &+ \frac{1}{2} \delta \left\{ \sum_{\mu=1}^P \sum_{\nu=1}^P \bar{y}'_\mu \left[ \frac{\partial^2 \bar{V}_{\text{eff}}}{\partial \bar{y}_\mu \partial \bar{y}_\nu} \right]_{\delta^{1/2}=0} \bar{y}'_\nu + v_o \right\} + O(\delta^{3/2}), \end{aligned} \quad (10)$$

where  $P = N(N+1)/2$  is the number of internal coordinates and  $v_o = \left[ \frac{\partial \bar{V}_{\text{eff}}}{\partial \delta} \right]_{\delta^{1/2}=0}$ . The derivative terms in the kinetic energy have a similar series expansion:

$$\mathcal{T} = -\frac{1}{2} \delta \sum_{\mu=1}^P \sum_{\nu=1}^P G_{\mu\nu} \partial_{\bar{y}'_\mu} \partial_{\bar{y}'_\nu} + O(\delta^{3/2}), \quad (11)$$

where  $\mathcal{T}$  is the derivative portion of the kinetic energy  $T$  (see Eq. (4)). Thus, determining the energy at first order is reduced to a harmonic problem, which is solved by obtaining the normal modes of the system. From Eqs. (10) and (11),  $\mathbf{G}$  and  $\mathbf{F}$ , both constant matrices, are defined in the first-order  $\delta = 1/D$  Hamiltonian below:

$$\hat{H}_1 = -\frac{1}{2} \partial_{\bar{\mathbf{y}}'}^T \mathbf{G} \partial_{\bar{\mathbf{y}}'} + \frac{1}{2} \bar{\mathbf{y}}'^T \mathbf{F} \bar{\mathbf{y}}' + v_o. \quad (12)$$

### D. FG Matrix Method for the Normal Mode Frequencies and Coordinates

The FG matrix method[35] is used to obtain the normal-mode vibrations and the harmonic-order energy correction. A review of the FG matrix method is presented in Appendix A of Ref. [20], but a brief summary is given below.

The  $b^{\text{th}}$  normal mode coordinate may be written as (Eq. (A9) Ref. [20])

$$[\mathbf{q}']_b = \mathbf{b}^T \bar{\mathbf{y}}', \quad (13)$$

where the coefficient vector  $\mathbf{b}$  satisfies the eigenvalue equation (Eq. (A10) Ref. [20])

$$\mathbf{F} \mathbf{G} \mathbf{b} = \lambda_b \mathbf{b} \quad (14)$$

with the resultant secular equation (Eq. (A11) Ref. [20])  $\det(\mathbf{F}\mathbf{G} - \lambda\mathbf{I}) = 0$ . The coefficient vector also satisfies the normalization condition (Eq. (A12) Ref. [20])  $\mathbf{b}^T \mathbf{G} \mathbf{b} = 1$ , and the frequencies are:  $\lambda_b = \bar{\omega}_b^2$  (Eq. (A3) Ref. [20]).

In an earlier paper[22], we solve these equations for the frequencies. The number of roots  $\lambda$  is equal to  $P \equiv N(N+1)/2$ . However, due to the  $S_N$  symmetry (see Ref. [36] and Appendix A), there is a simplification to only five distinct roots,  $\lambda_\mu$ , where  $\mu$  runs over  $\mathbf{0}^-$ ,  $\mathbf{0}^+$ ,  $\mathbf{1}^-$ ,  $\mathbf{1}^+$ , and  $\mathbf{2}$ , (see Refs. [22, 37]). Thus the energy through first-order in  $\delta = 1/D$  (see Eq. (15)) can be written in terms of the five distinct normal-mode vibrational frequencies[22].

$$\bar{E} = \bar{E}_\infty + \delta \left[ \sum_{\mu=\{\mathbf{0}^\pm, \mathbf{1}^\pm, \mathbf{2}\}} (n_\mu + \frac{1}{2}d_\mu) \bar{\omega}_\mu + v_o \right]. \quad (15)$$

where  $\bar{E}_\infty$  is the energy minimum as  $\delta \rightarrow 0$ ,  $n_\mu$  is the total number of quanta in the normal mode with the frequency  $\bar{\omega}_\mu$ ;  $\mu$  is a label which runs over the five types of normal modes,  $\mathbf{0}^-$ ,  $\mathbf{0}^+$ ,  $\mathbf{1}^-$ ,  $\mathbf{1}^+$ , and  $\mathbf{2}$ , (irrespective of the particle number, see Ref. [22] and Ref.[15] in [20]), and  $v_o$  is a constant (defined above and in Ref. [22], Eq. 125). The multiplicities of the five roots are:  $d_{\mathbf{0}^+} = 1$ ,  $d_{\mathbf{0}^-} = 1$ ,  $d_{\mathbf{1}^+} = N-1$ ,  $d_{\mathbf{1}^-} = N-1$ ,  $d_{\mathbf{2}} = N(N-3)/2$ .

### E. Symmetry of the $\mathbf{F}$ , $\mathbf{G}$ and $\mathbf{FG}$ Matrices

The large degeneracy of the frequencies indicates a very high degree of symmetry which is manifested in the  $\mathbf{F}$ ,  $\mathbf{G}$ , and  $\mathbf{FG}$  matrices which are  $P \times P$  matrices. The  $S_N$  symmetry of these matrices, whose elements are evaluated for the maximally symmetric structure at large dimension, allows them to be written in terms of six simple submatrices which are invariant under  $S_N$  (See Ref [22]). The number of  $r_i$  coordinates is  $N$  and the number of  $\gamma_{ij}$  coordinates is  $N(N-1)/2$ . These matrices are invariant under interchange of the particles, effected by the point group  $S_N$ [22].

We can thus write the  $\mathbf{F}$ ,  $\mathbf{G}$  and  $\mathbf{FG}$  matrices with the following structure:

$$\mathbf{F} = \begin{pmatrix} \mathbf{F}_{\bar{\mathbf{r}}' \bar{\mathbf{r}}'} & \mathbf{F}_{\bar{\mathbf{r}}' \bar{\boldsymbol{\gamma}}'} \\ \mathbf{F}_{\bar{\boldsymbol{\gamma}}' \bar{\mathbf{r}}'} & \mathbf{F}_{\bar{\boldsymbol{\gamma}}' \bar{\boldsymbol{\gamma}}'} \end{pmatrix} \quad \mathbf{G} = \begin{pmatrix} \mathbf{G}_{\bar{\mathbf{r}}' \bar{\mathbf{r}}'} & \mathbf{G}_{\bar{\mathbf{r}}' \bar{\boldsymbol{\gamma}}'} \\ \mathbf{G}_{\bar{\boldsymbol{\gamma}}' \bar{\mathbf{r}}'} & \mathbf{G}_{\bar{\boldsymbol{\gamma}}' \bar{\boldsymbol{\gamma}}'} \end{pmatrix} \quad (16)$$

$$\mathbf{FG} = \begin{pmatrix} \mathbf{FG}_{\bar{\mathbf{r}}' \bar{\mathbf{r}}'} & \mathbf{FG}_{\bar{\mathbf{r}}' \bar{\boldsymbol{\gamma}}'} \\ \mathbf{FG}_{\bar{\boldsymbol{\gamma}}' \bar{\mathbf{r}}'} & \mathbf{FG}_{\bar{\boldsymbol{\gamma}}' \bar{\boldsymbol{\gamma}}'} \end{pmatrix} \quad (17)$$

The structure of these matrices results in highly degenerate eigenvalues and causes a reduction from a possible  $P = N(N+1)/2$  distinct frequencies to just five distinct frequencies for  $L = 0$  systems.

### F. Symmetry Coordinates

The  $\mathbf{FG}$  matrix is invariant under  $S_N$ , so it does not connect subspaces belonging to different irreducible rep-

resentations of  $S_N$ [38]. Thus from Eqs. (13) and (14) the normal coordinates must transform under irreducible representations of  $S_N$ . The normal coordinates will be linear combinations of the elements of the internal coordinate displacement vectors  $\bar{\mathbf{r}}'$  and  $\bar{\boldsymbol{\gamma}}'$  which transform under reducible matrix representations of  $S_N$ , each spanning the corresponding carrier spaces. (Appendix A).

The radial displacement coordinate  $\bar{\mathbf{r}}'$  transforms under a reducible representation that reduces to one 1-dimensional irreducible representation labelled by the partition  $[N]$  (the partition denotes a corresponding Young diagram of an irreducible representation (see Appendix A)) and one  $(N-1)$ -dimensional irreducible representation labelled by the partition  $[N-1, 1]$ . The angular displacement coordinate  $\bar{\boldsymbol{\gamma}}'$  transforms under a reducible representation that reduces to one 1-dimensional irreducible representation labelled by the partition  $[N]$ , one  $(N-1)$ -dimensional irreducible representation labelled by the partition  $[N-1, 1]$  and one  $N(N-3)/2$ -dimensional irreducible representation labelled by the partition  $[N-2, 2]$ .

We define the symmetry coordinate vector,  $S$  as:

$$S = \begin{pmatrix} S_{\bar{\mathbf{r}}'}^{[N]} \\ S_{\bar{\boldsymbol{\gamma}}'}^{[N]} \\ S_{\bar{\mathbf{r}}'}^{[N-1, 1]} \\ S_{\bar{\boldsymbol{\gamma}}'}^{[N-1, 1]} \\ S_{\bar{\boldsymbol{\gamma}}'}^{[N-2, 2]} \end{pmatrix} = \begin{pmatrix} W_{\bar{\mathbf{r}}'}^{[N]} \bar{\mathbf{r}}' \\ W_{\bar{\boldsymbol{\gamma}}'}^{[N]} \bar{\boldsymbol{\gamma}}' \\ W_{\bar{\mathbf{r}}'}^{[N-1, 1]} \bar{\mathbf{r}}' \\ W_{\bar{\boldsymbol{\gamma}}'}^{[N-1, 1]} \bar{\boldsymbol{\gamma}}' \\ W_{\bar{\boldsymbol{\gamma}}'}^{[N-2, 2]} \bar{\boldsymbol{\gamma}}' \end{pmatrix}, \quad (18)$$

where the  $W_{\bar{\mathbf{r}}'}^{[\alpha]}$  and the  $W_{\bar{\boldsymbol{\gamma}}'}^{[\alpha]}$  are the transformation matrices. This is shown in Ref. [20] using the theory of group characters to decompose  $\bar{\mathbf{r}}'$  and  $\bar{\boldsymbol{\gamma}}'$  into basis functions that transform under these five irreducible representations of  $S_N$ .

The process used in Ref. [20] to determine the symmetry coordinates, and hence the  $W_{\bar{\mathbf{r}}'}^{[\alpha]}$  and  $W_{\bar{\boldsymbol{\gamma}}'}^{[\alpha]}$  matrices was chosen to ensure that the  $W$  matrices satisfy the orthogonality restrictions between different irreducible representations. This process also ensured that the sets of coordinates transforming irreducibly under  $S_N$  have the simplest functional forms possible. One of the symmetry coordinates was chosen to describe the simplest motion possible under the requirement that it transforms irreducibly under  $S_N$ . The succeeding symmetry coordinate was then chosen to have the next simplest possible functional form that transforms irreducibly under  $S_N$  etc. In this way the complexity of the motions described by the symmetry coordinates was minimized, building up slowly as more symmetry coordinates of a given species were added as  $N$  increased, with no disruption of lower  $N$  symmetry coordinates. This method of determining the symmetry coordinate basis is not unique, but was chosen to minimize the complexity.

### G. Symmetry Coordinates and Transformation Matrices

The five transformation matrices and the symmetry coordinates for five irreducible representations are:

$$[W_{\bar{\mathbf{r}}'}^{[N]}]_i = \frac{1}{\sqrt{N}} [\mathbf{1}_{\bar{\mathbf{r}}'}]_i, \quad \mathbf{S}_{\bar{\mathbf{r}}'}^{[N]} = \frac{1}{\sqrt{N}} \sum_{i'=1}^N \bar{\mathbf{r}}'_{i'}. \quad (19)$$

$$[W_{\bar{\gamma}'}^{[N]}]_{ij} = \sqrt{\frac{2}{N(N-1)}} [\mathbf{1}_{\bar{\gamma}'}]_{ij} \quad (20)$$

$$\text{and } \mathbf{S}_{\bar{\gamma}'}^{[N]} = \sqrt{\frac{2}{N(N-1)}} \sum_{j'=2}^N \sum_{i' < j'} \bar{\gamma}'_{i'j'}. \quad (21)$$

where  $[\mathbf{1}_{\bar{\mathbf{r}}'}]_i = 1 \ \forall \ 1 \leq i \leq N$  and  $[\mathbf{1}_{\bar{\gamma}'}]_{ij} = 1 \ \forall \ 1 \leq i, j \leq N$ .

$$[W_{\bar{\mathbf{r}}'}^{[N-1, 1]}]_{\xi i} = \frac{1}{\sqrt{\xi(\xi+1)}} \left( \sum_{m=1}^{\xi} \delta_{mi} - \xi \delta_{\xi+1, i} \right) \quad (22)$$

$$[\mathbf{S}_{\bar{\mathbf{r}}'}^{[N-1, 1]}]_{\xi} = \frac{1}{\sqrt{\xi(\xi+1)}} \left( \sum_{k'=1}^{\xi} \bar{\mathbf{r}}'_{k'} - \xi \bar{\mathbf{r}}'_{\xi+1} \right), \quad (23)$$

where  $1 \leq \xi \leq N-1$  and  $1 \leq i \leq N$ .

$$\begin{aligned} [W_{\bar{\gamma}'}^{[N-1, 1]}]_{\xi, ij} &= \frac{1}{\sqrt{\xi(\xi+1)(N-2)}} \left( (\Theta_{\xi-i+1} [\mathbf{1}_{\bar{\mathbf{r}}'}]_j + \Theta_{\xi-j+1} [\mathbf{1}_{\bar{\mathbf{r}}'}]_i) - \xi (\delta_{\xi+1, i} [\mathbf{1}_{\bar{\mathbf{r}}'}]_j + \delta_{\xi+1, j} [\mathbf{1}_{\bar{\mathbf{r}}'}]_i) \right), \\ [\mathbf{S}_{\bar{\gamma}'}^{[N-1, 1]}]_{\xi} &= \frac{1}{\sqrt{\xi(\xi+1)(N-2)}} \left( \left[ \sum_{l'=2}^{\xi} \sum_{k'=1}^{l'-1} \bar{\gamma}'_{k'l'} + \sum_{k'=1}^{\xi} \sum_{l'=k'+1}^N \bar{\gamma}'_{k'l'} \right] - \xi \left[ \sum_{k'=1}^{\xi} \bar{\gamma}'_{k', \xi+1} + \sum_{l'=\xi+2}^N \bar{\gamma}'_{\xi+1, l'} \right] \right). \end{aligned} \quad (24)$$

where  $1 \leq \xi \leq N-1$  and  $1 \leq i < j \leq N$ .

$$\begin{aligned} [W_{\bar{\gamma}'}^{[N-2, 2]}]_{ij, mn} &= \frac{1}{\sqrt{i(i+1)(j-3)(j-2)}} \left( (\Theta_{i-m+1} - i\delta_{i+1, m})(\Theta_{j-n} - (j-3)\delta_{jn}) + (\Theta_{i-n+1} - i\delta_{i+1, n}) \right. \\ &\quad \left. \times (\Theta_{j-m} - (j-3)\delta_{jm}) \right) \\ [\mathbf{S}_{\bar{\gamma}'}^{[N-2, 2]}]_{ij} &= \frac{1}{\sqrt{i(i+1)(j-3)(j-2)}} \left( \sum_{j'=2}^{j-1} \sum_{k=1}^{[j'-1, i]_{min}} \bar{\gamma}'_{kj'} + \sum_{k=1}^{i-1} \sum_{j'=k+1}^i \bar{\gamma}'_{kj'} - (j-3) \sum_{k=1}^i \bar{\gamma}'_{kj} \right. \\ &\quad \left. - i \sum_{k=1}^i \bar{\gamma}'_{k, (i+1)} - i \sum_{j'=i+2}^{j-1} \bar{\gamma}'_{(i+1), j'} + i(j-3) \bar{\gamma}'_{(i+1), j} \right), \end{aligned} \quad (25)$$

where  $1 \leq i \leq j-2$  and  $4 \leq j \leq N$  and  $1 \leq m < n \leq N$ . We define the Heaviside step function as:

$$\begin{aligned} \Theta_{i-j+1} &= \sum_{m=1}^i \delta_{mj} = 1 \text{ when } j-i < 1 \\ &= 0 \text{ when } j-i \geq 1. \end{aligned} \quad (26)$$

### H. Transformation to Normal Mode Coordinates

The invariance of Eq. (13) under  $S_N$  means that the F, G and FG matrices used to solve for the first-order energies and normal modes transform under irreducible representations of  $S_N$ . When the FG matrix is transformed from the  $\bar{\mathbf{r}}'$  and  $\bar{\gamma}'$  basis to symmetry coordinates, the full  $N(N+1)/2 \times N(N+1)/2$  matrix is reduced to block diagonal form yielding one  $2 \times 2$  block for the  $[N]$  sector,  $N-1$  identical  $2 \times 2$  blocks for the  $[N-1, 1]$  sector and  $N(N-3)/2$  identical  $1 \times 1$  blocks for the  $[N-2, 2]$  sector.

In the  $[N]$  and  $[N-1, 1]$  sectors, the  $2 \times 2$  blocks allow

the  $\bar{\mathbf{r}}'$  and  $\bar{\gamma}'$  symmetry coordinates to mix in the normal coordinates. The  $1 \times 1$  structure in the  $[N-2, 2]$  sector reflects the fact that the  $[N-2, 2]$  normal modes are entirely angular i.e. there are no  $\bar{\mathbf{r}}'$  symmetry coordinates in this sector.

We applied the **FG** method using these symmetry coordinates to determine the eigenvalues,  $\lambda_\alpha = \bar{\omega}_\alpha^2$ , frequencies,  $\bar{\omega}_\alpha$  and normal modes,  $\mathbf{q}'$  of the system:

$$\lambda_\alpha^\pm = \frac{a_\alpha \pm \sqrt{b_\alpha^2 + 4c_\alpha}}{2} \quad (27)$$

for the  $\alpha = [N]$  and  $[N-1, 1]$  sectors, where

$$\begin{aligned} a_\alpha &= [\sigma_\alpha^{FG}]_{\bar{\mathbf{r}}', \bar{\mathbf{r}}'} + [\sigma_\alpha^{FG}]_{\bar{\gamma}', \bar{\gamma}'} \\ b_\alpha &= [\sigma_\alpha^{FG}]_{\bar{\mathbf{r}}', \bar{\gamma}'} - [\sigma_\alpha^{FG}]_{\bar{\gamma}', \bar{\mathbf{r}}'} \\ c_\alpha &= [\sigma_\alpha^{FG}]_{\bar{\mathbf{r}}', \bar{\gamma}'} \times [\sigma_\alpha^{FG}]_{\bar{\gamma}', \bar{\mathbf{r}}'}, \end{aligned} \quad (28)$$

while  $\lambda_{[N-2, 2]} = \sigma_{[N-2, 2]}^{FG}$ . The  $\sigma_\alpha^{FG}$  are the elements of the **FG** matrix of Eq. (17) expressed in the basis of symmetry coordinates. The  $\sigma_\alpha^{FG}$  for the  $\alpha = [N]$  and  $[N-1, 1]$  sectors are  $2 \times 2$  matrices (See Appendix B), while  $\sigma_{[N-2, 2]}^{FG}$  is a one-component quantity. These quantities are defined generally in Ref. [20] Eqs. (28, 29, 126, 162, 163) and also specifically in Ref. [22] for three different confining and interparticle potentials. The normal coordinates are:

$$\mathbf{q}'_{\pm}^{[N]} = c_{\pm}^{[N]} \left( \cos \theta_{\pm}^{[N]} [\mathbf{S}_{\bar{\mathbf{r}}'}^{[N]}] + \sin \theta_{\pm}^{[N]} [\mathbf{S}_{\bar{\gamma}'}^{[N]}] \right) \quad (29)$$

$$\begin{aligned} \mathbf{q}'_{\xi\pm}^{[N-1, 1]} &= c_{\pm}^{[N-1, 1]} \left( \cos \theta_{\pm}^{[N-1, 1]} [\mathbf{S}_{\bar{\mathbf{r}}'}^{[N-1, 1]}]_{\xi} \right. \\ &\quad \left. + \sin \theta_{\pm}^{[N-1, 1]} [\mathbf{S}_{\bar{\gamma}'}^{[N-1, 1]}]_{\xi} \right) \end{aligned} \quad (30)$$

for the  $\alpha = [N]$  and  $[N-1, 1]$  sectors,  $1 \leq \xi \leq N-1$  and

$$\mathbf{q}'^{[N-2, 2]} = c^{[N-2, 2]} \mathbf{S}_{\bar{\gamma}'}^{[N-2, 2]} \quad (31)$$

for the  $[N-2, 2]$  sector. The  $\bar{\mathbf{r}}'$ - $\bar{\gamma}'$  mixing angle,  $\theta_{\pm}^\alpha$ , is given by

$$\tan \theta_{\pm}^\alpha = \frac{(\lambda_{\pm}^\alpha - [\sigma_\alpha^{FG}]_{\bar{\mathbf{r}}', \bar{\mathbf{r}}'})}{[\sigma_\alpha^{FG}]_{\bar{\mathbf{r}}', \bar{\gamma}'}} = \frac{[\sigma_\alpha^{FG}]_{\bar{\gamma}', \bar{\mathbf{r}}'}}{(\lambda_{\pm}^\alpha - [\sigma_\alpha^{FG}]_{\bar{\gamma}', \bar{\gamma}'}),} \quad (32)$$

while the normalization constants  $c^{[\alpha]}$  are given by

$$c_{\pm}^{[\alpha]} = \frac{1}{\sqrt{\left( \begin{pmatrix} \cos \theta_{\pm}^{[\alpha]} \\ \sin \theta_{\pm}^{[\alpha]} \end{pmatrix}^T \sigma_\alpha^G \begin{pmatrix} \cos \theta_{\pm}^{[\alpha]} \\ \sin \theta_{\pm}^{[\alpha]} \end{pmatrix} \right)}} \quad (33)$$

$$c^{[N-2, 2]} = \frac{1}{\sqrt{\sigma_{[N-2, 2]}^G}}. \quad (34)$$

The  $\sigma_\alpha^G$  are related to the elements of the **G** matrix of Eq. (12). One determines the  $\bar{\mathbf{r}}'$ - $\bar{\gamma}'$  mixing angles,  $\theta_{\pm}^{[\alpha]}$  for the  $[N]$  and  $[N-1, 1]$  species from Eq. (32). The normalization constants  $c^{[\alpha]}$  of Eqs. (29) and (31) are determined from Eqs. (32) (33) and (34). The normal mode vector,  $\mathbf{q}'$ , is then determined through Eqs. (29) and (31). The analytic normal coordinates for  $N$  identical particles are:

$$\begin{aligned} \mathbf{q}'_{\pm}^{[N]} &= c_{\pm}^{[N]} \cos \theta_{\pm}^{[N]} \frac{1}{\sqrt{N}} \sum_{i'=1}^N \bar{\mathbf{r}}'_{i'} + c_{\pm}^{[N]} \sin \theta_{\pm}^{[N]} \sqrt{\frac{2}{N(N-1)}} \sum_{j'=2}^N \sum_{i' < j'} \bar{\gamma}'_{i'j'}, \\ [\mathbf{q}'_{\pm}^{[N-1, 1]}]_{\xi} &= c_{\pm}^{[N-1, 1]} \cos \theta_{\pm}^{[N-1, 1]} \frac{1}{\sqrt{\xi(\xi+1)}} \left( \sum_{k'=1}^{\xi} \bar{\mathbf{r}}'_{k'} - \xi \bar{\mathbf{r}}'_{\xi+1} \right) + c_{\pm}^{[N-1, 1]} \sin \theta_{\pm}^{[N-1, 1]} \frac{1}{\sqrt{\xi(\xi+1)(N-2)}} \\ &\quad \left( \left[ \sum_{l'=2}^{\xi} \sum_{k'=1}^{l'-1} \bar{\gamma}'_{k'l'} + \sum_{k'=1}^{\xi} \sum_{l'=k'+1}^N \bar{\gamma}'_{k'l'} \right] - \xi \left[ \sum_{k'=1}^{\xi} \bar{\gamma}'_{k', \xi+1} + \sum_{l'=\xi+2}^N \bar{\gamma}'_{\xi+1, l'} \right] \right) \end{aligned}$$

where  $1 \leq \xi \leq N-1$ ,

$$\begin{aligned} [\mathbf{q}'^{[N-2, 2]}]_{ij} &= c^{[N-2, 2]} \frac{1}{\sqrt{i(i+1)(j-3)(j-2)}} \left( \sum_{j'=2}^{j-1} \sum_{k=1}^{[j'-1, i]_{\min}} \bar{\gamma}'_{kj'} + \sum_{k=1}^{i-1} \sum_{j'=k+1}^i \bar{\gamma}'_{kj'} - (j-3) \sum_{k=1}^i \bar{\gamma}'_{kj} \right. \\ &\quad \left. - i \sum_{k=1}^i \bar{\gamma}'_{k, (i+1)} - i \sum_{j'=i+2}^{j-1} \bar{\gamma}'_{(i+1), j'} + i(j-3) \bar{\gamma}'_{(i+1), j} \right), \end{aligned}$$

where  $1 \leq i \leq j-2$  and  $4 \leq j \leq N$

### III. MOTIONS ASSOCIATED WITH THE SYMMETRY COORDINATES

In this section, I analyze the motions of the five types of symmetry coordinates as expressed in Eqs. (19, 21,

23 - 25). For symmetry coordinates, there is no mixing of radial and angular motion, so the motion is either totally radial or totally angular. The symmetry coordinates transform irreducibly under  $S_N$  and result in a block diagonal form for the  $H_0$  matrix. When these blocks are diagonalized we obtain the normal coordinates which are the solutions to the first order equation. For the  $[N]$  and  $[N - 1, 1]$  sectors which are found in both the radial and angular decompositions, there is mixing of these radial and angular symmetry coordinates in the normal modes. For the  $[N - 2, 2]$  sector, there is no radial part, only an angular part, so no mixing; the symmetry coordinates are the normal coordinates apart from a normalization constant.

The symmetry coordinates describe motion that is collective with the particles participating in synchronized motion, i.e. moving with the same frequency and phase. Since the symmetry coordinates, except for the  $[N - 2, 2]$  modes, are not solutions to the Hamiltonian at first order, they do not necessarily exhibit the motion of particles governed by the Hamiltonian. Their motions could be mixed significantly with another symmetry coordinate of the same species to form a normal coordinate, a solution to the Hamiltonian at first order. I will analyze the motion of the symmetry coordinates first and then use the knowledge of these motions to understand the normal coordinate behavior.

I am interested in the motion of individual particles as they participate in the collective synchronized motion of these symmetry coordinates. To determine the motion of an individual particle, I need to back transform from the known functional form of a particular symmetry coordinate to the scaled internal displacement coordinates,  $\bar{r}'_i$  and  $\bar{\gamma}'_{ij}$  and then transform from the scaled to the unscaled displacement coordinates to be able to visualize these displacements. Using Eq.(19) I can obtain the dimensionally scaled  $\bar{\mathbf{r}}'$  and  $\bar{\boldsymbol{\gamma}}'$  vectors by back transforming with the transpose of the  $W$  matrices. These dimensionally scaled variables can be transformed to the unscaled internal displacement coordinates using  $\bar{r}_i = \bar{r}_\infty + \delta^{1/2}\bar{r}'_i$ ,  $\gamma_{ij} = \bar{\gamma}_\infty + \delta^{1/2}\bar{\gamma}'_{ij}$  and  $r_i = \kappa(D)\bar{r}_i$ . The unscaled internal coordinates,  $r_i$  and  $\gamma_{ij}$ , allow one to determine the radial distance from the confinement center and the interparticle angle of each pair of particles using  $\gamma_{ij} = \cos \theta_{ij}$  and  $\bar{\gamma}_\infty = \cos \theta_\infty$ , so  $\theta_{ij} = \arccos \gamma_{ij}$  and  $\theta_\infty = \arccos \bar{\gamma}_\infty$ . Then  $r_i - r_\infty$  and  $\theta_{ij} - \theta_\infty$  give displacements from the maximally symmetric zeroth-order configuration  $(r_\infty, \gamma_\infty)$  that are easy to visualize, connecting to our physical intuition and thus contributing to our understanding of how the motion of  $N$  particles becomes collective.

*a. Motions Associated with Symmetry Coordinate  $\mathbf{S}_{\bar{\mathbf{r}}'}^{[N]}$ .* The simplest collective motion for a system of identical particles occurs when every particle executes the same motion with the same phase. This type of collective motion occurs for the symmetry coordinates of the  $[N]$  modes, both the radial symmetry coordinate  $\mathbf{S}_{\bar{\mathbf{r}}'}^{[N]}$  and

angular symmetry coordinate  $\mathbf{S}_{\bar{\boldsymbol{\gamma}}'}^{[N]}$ . There is just one symmetry coordinate in each  $[N]$  sector. I am interested in the unscaled displacement quantity  $\mathbf{r}'_i = \kappa(D)\bar{r}'_i = D^2\bar{a}_{ho}\bar{r}'_i$ . For the  $[N]$  symmetry coordinate  $\mathbf{S}_{\bar{\mathbf{r}}'}^{[N]}$ ,  $\bar{r}'_i$  is obtained by back transforming with  $W_{\bar{\mathbf{r}}'}^{[N]}$ . Using Eqs. (18) and (19) the motions associated with symmetry coordinate  $\mathbf{S}_{\bar{\mathbf{r}}'}^{[N]}$  in the unscaled internal displacement coordinates  $\mathbf{r}'$  about the unscaled zeroth-order configuration  $\mathbf{r}_\infty$  are given by:

$$\mathbf{r}'^{[N]} = \bar{a}_{ho} D^2 \bar{\mathbf{r}}'^{[N]} = \bar{a}_{ho} D^2 [(W_{\bar{\mathbf{r}}'}^{[N]})^T \mathbf{S}_{\bar{\mathbf{r}}'}^{[N]}] \quad (35)$$

$$= \bar{a}_{ho} \frac{D^2}{\sqrt{N}} \mathbf{S}_{\bar{\mathbf{r}}'}^{[N]} \mathbf{1}_{\bar{\mathbf{r}}'}. \quad (36)$$

The vector  $\mathbf{r}'^{[N]}$  is a  $N \times 1$  vector of the unscaled radial displacement coordinates for all the particles participating in this collective motion. The motions of all the particles are thus identical in this symmetry coordinate  $\mathbf{S}_{\bar{\mathbf{r}}'}^{[N]}$  involving identical radial motions out and then back in from the positions of the zeroth-order configuration. This results in a symmetric stretch collective motion, where all the radii expand and contract together with decreasing amplitudes as  $N$  increases. For  $N = 3$ , a good molecular comparison is the stretching  $A_1$  mode of ammonia.

*b. Motions Associated with Symmetry Coordinate  $\mathbf{S}_{\bar{\boldsymbol{\gamma}}'}^{[N]}$ .* Using Eqs. (18) and (20), the motions associated with symmetry coordinate  $\mathbf{S}_{\bar{\boldsymbol{\gamma}}'}^{[N]}$  in the unscaled internal displacement coordinates  $\boldsymbol{\gamma}'$  about the zeroth-order configuration  $\boldsymbol{\gamma}_\infty$  are given by

$$\boldsymbol{\gamma}'^{[N]} = [(W_{\bar{\boldsymbol{\gamma}}'}^{[N]})^T \mathbf{S}_{\bar{\boldsymbol{\gamma}}'}^{[N]}] \quad (37)$$

$$= \sqrt{\frac{2}{N(N-1)}} \mathbf{S}_{\bar{\boldsymbol{\gamma}}'}^{[N]} \mathbf{1}_{\bar{\boldsymbol{\gamma}}'}. \quad (38)$$

This vector  $\boldsymbol{\gamma}'^{[N]}$  is a  $N(N-1)/2 \times 1$  vector of the displacement contributions to the angle cosines for all the particles participating in this collective motion. The motions of all the particles are thus identical in this symmetry coordinate  $\mathbf{S}_{\bar{\boldsymbol{\gamma}}'}^{[N]}$  involving identical angular motions for each pair of particles from the interparticle angles of the zeroth-order configuration. This results in a symmetric bend collective motion, where all of the interparticle angles expand and contract together with the radii unchanged. For  $N = 3$ , a good molecular comparison is the bending  $A_1$  mode of ammonia. As  $N$  increases this symmetric bending motion evolves into a center of mass motion with small angular displacements for every interparticle angle while the radii remain fixed. (See Section V A for more detail.)

*c. Motions Associated with Symmetry Coordinates  $[\mathbf{S}_{\bar{\mathbf{r}}'}^{[N-1, 1]}]_\xi$ .* Using Eqs. (18), (22), and (26) the motions associated with symmetry coordinates  $[\mathbf{S}_{\bar{\mathbf{r}}'}^{[N-1, 1]}]_\xi$  in the unscaled internal displacement coordinates  $\mathbf{r}'$  about the unscaled zeroth-order configuration  $\mathbf{r}_\infty$  are



given by

$$\begin{aligned}
(r_\xi'^{[N-1, 1]})_i &= \bar{a}_{ho} D^2 (\bar{r}_\xi'^{[N-1, 1]})_i \\
&= \bar{a}_{ho} D^2 [\mathbf{S}_{\bar{\mathbf{r}}'}^{[N-1, 1]}]_\xi [(W_{\bar{\mathbf{r}}'}^{[N-1, 1]})_\xi]_i \\
&= \bar{a}_{ho} \frac{D^2}{\sqrt{\xi(\xi+1)}} [\mathbf{S}_{\bar{\mathbf{r}}'}^{[N-1, 1]}]_\xi \\
&\quad \times (\Theta_{\xi-i+1} - \xi \delta_{\xi+1, i}).
\end{aligned} \tag{39}$$

The above equation gives the radial motion of the  $i^{th}$  particle participating in the collective motion of the  $\xi^{th}$  symmetry coordinate in the radial  $[N-1, 1]$  sector. In this sector there are  $N-1$  radial symmetry coordinates i.e.  $1 \leq \xi \leq N-1$ , and the  $\xi^{th}$  symmetry coordinate involves the motion of the first  $\xi+1$  particles. (If  $i > \xi+1$ , the Heaviside and Kronecker delta functions are zero in Eq. 39). Thus the motion associated with symmetry coordinate  $[\mathbf{S}_{\bar{\mathbf{r}}'}^{[N-1, 1]}]_1$  is an antisymmetric stretch about

the zeroth-order configuration involving particles 1 and 2. As  $\xi$  gets larger, the motion involves more particles,  $\xi+1$  particles, with the first  $\xi$  particles moving one way while the  $(\xi+1)^{th}$  particle moves the other way. As  $\xi$  increases, the character of the motion evolves from an antisymmetric stretch motion (a good molecular equivalent is an  $E$  mode of ammonia), to behavior that becomes more single-particle-like, i.e. a particle-hole excitation associated with radial motion, since the  $(\xi+1)^{th}$  radius vector in Eq. (39) is weighted by the quantity  $\xi$ . (I examine this dependence on the number of particles as  $N$  increases in more detail in Section V A.)

*d. Motions Associated with Symmetry Coordinates*  $[\mathbf{S}_{\bar{\mathbf{r}}'}^{[N-1, 1]}]_\xi$ . Using Eqs. (18) and (24), the motions associated with symmetry coordinates  $[\mathbf{S}_{\bar{\mathbf{r}}'}^{[N-1, 1]}]_\xi$  in the unscaled internal displacement coordinates  $\gamma'$  about the unscaled zeroth-order configuration  $\gamma_\infty = \gamma_\infty \mathbf{1}_{\bar{\mathbf{r}}'}$  are given by:

$$\begin{aligned}
(\gamma_\xi'^{[N-1, 1]})_{ij} &= [\mathbf{S}_{\bar{\mathbf{r}}'}^{[N-1, 1]}]_\xi [(W_{\bar{\mathbf{r}}'}^{[N-1, 1]})_\xi]_{ij} = \frac{1}{\sqrt{\xi(\xi+1)(N-2)}} [\mathbf{S}_{\bar{\mathbf{r}}'}^{[N-1, 1]}]_\xi \\
&\quad \times \left( (\Theta_{\xi-i+1} [\mathbf{1}_{\bar{\mathbf{r}}'}]_{ij} + \Theta_{\xi-j+1} [\mathbf{1}_{\bar{\mathbf{r}}'}]_{ij}) - \xi (\delta_{\xi+1, i} [\mathbf{1}_{\bar{\mathbf{r}}'}]_{ij} + \delta_{\xi+1, j} [\mathbf{1}_{\bar{\mathbf{r}}'}]_{ij}) \right).
\end{aligned} \tag{40}$$

The above equation gives the angular displacement of the  $i^{th}$  and  $j^{th}$  particles participating in the collective motion of the  $\xi$  symmetry coordinate in the angular  $[N-1, 1]$  sector. The  $\xi^{th}$  symmetry coordinate in this angular sector  $[N-1, 1]$  involves the angular motion of the first  $\xi+1$  particles, thus affecting any angular displacement  $\gamma_{ij}$  where  $1 \leq i \leq \xi+1$  or  $1 \leq j \leq \xi+1$ . All other angular displacements are zero. (When  $i, j > \xi+1$ , the Heaviside and Kronecker delta functions are zero. The  $\gamma_{12}$  displacement is zero by cancellation.) Thus the motion associated with symmetry coordinate  $[\mathbf{S}_{\bar{\mathbf{r}}'}^{[N-1, 1]}]_1$  is an antisymmetric bending about the zeroth-order configuration where the angle cosines  $\gamma'_{13}, \gamma'_{14}, \gamma'_{15}, \dots$  increase,  $\gamma'_{23}, \gamma'_{24}, \gamma'_{25}, \dots$  decrease while  $\gamma'_{12}, \gamma'_{34}, \gamma'_{35}, \gamma'_{45}, \dots$  remain unchanged. Thus, analogously to the  $\bar{\mathbf{r}}'$  sector of the  $[N-1, 1]$  species,  $[\mathbf{S}_{\bar{\mathbf{r}}'}^{[N-1, 1]}]_1$  involves the motions of particles 1 and 2 moving with opposite phase to each

other. As  $\xi$  gets larger, the angular motion involves more particles,  $\xi+1$  particles, with the  $(\xi+1)^{th}$  particle moving with opposite phase to the first  $\xi$  particles. Analogously to the radial sector of the  $[N-1, 1]$  species, as  $\xi$  increases the motion evolves from an antisymmetric stretch motion (cf. an  $E$  mode of ammonia), to behavior that becomes more single-particle-like, i.e. a particle-hole excitation due to angular displacement, since the angle cosines involving the  $(\xi+1)^{th}$  particle in Eq. (40) are weighted by the quantity  $\xi$ .

*e. Motions Associated with Symmetry Coordinate*  $[\mathbf{S}_{\bar{\mathbf{r}}'}^{[N-2, 2]}]_{ij}$ . Using Eqs. (18) and (25), the motions of the unscaled internal displacement coordinates  $\gamma'$  about the unscaled zeroth-order configuration  $\gamma_\infty = \gamma_\infty \mathbf{1}_{\bar{\mathbf{r}}'}$  associated with the symmetry coordinates  $[\mathbf{S}_{\bar{\mathbf{r}}'}^{[N-2, 2]}]_{ij}$  are given by:

$$\begin{aligned}
(\gamma_{ij}'^{[N-2, 2]})_{mn} &= [\mathbf{S}_{\bar{\mathbf{r}}'}^{[N-2, 2]}]_{ij} [W_{\bar{\mathbf{r}}'}^{[N-2, 2]}]_{ij, mn} = \frac{1}{\sqrt{i(i+1)(j-3)(j-2)}} [\mathbf{S}_{\bar{\mathbf{r}}'}^{[N-2, 2]}]_{ij} \\
&\quad \times \left( (\Theta_{i-m+1} - i\delta_{i+1, m})(\Theta_{j-n} - (j-3)\delta_{jn}) + (\Theta_{i-n+1} - i\delta_{i+1, n})(\Theta_{j-m} - (j-3)\delta_{jm}) \right),
\end{aligned} \tag{41}$$

where  $1 \leq m < n \leq N$ , and  $1 \leq i \leq j-2$  and  $4 \leq j \leq N$ . The above equation gives the angu-

lar displacement (contribution to the angle cosine) of the  $m^{th}$  and  $n^{th}$  particles participating in the collective motion of the  $ij^{th}$  symmetry coordinate in the  $[N-2, 2]$  sector. There are  $N(N-3)/2$  symmetry coordinates  $[\mathbf{S}_{\overline{\gamma}}^{[N-2, 2]}]_{ij}$  in this sector labeled by  $[\mathbf{S}_{\overline{\gamma}}^{[N-2, 2]}]_{14}$ ,  $[\mathbf{S}_{\overline{\gamma}}^{[N-2, 2]}]_{24}$ ,  $[\mathbf{S}_{\overline{\gamma}}^{[N-2, 2]}]_{15}$ ,  $[\mathbf{S}_{\overline{\gamma}}^{[N-2, 2]}]_{25}$ ,  $[\mathbf{S}_{\overline{\gamma}}^{[N-2, 2]}]_{35}$ ,  $[\mathbf{S}_{\overline{\gamma}}^{[N-2, 2]}]_{16}$ ,  $[\mathbf{S}_{\overline{\gamma}}^{[N-2, 2]}]_{26}$ ,  $[\mathbf{S}_{\overline{\gamma}}^{[N-2, 2]}]_{36}$ ,  $[\mathbf{S}_{\overline{\gamma}}^{[N-2, 2]}]_{46}$ ,  $[\mathbf{S}_{\overline{\gamma}}^{[N-2, 2]}]_{17}$ ,  $\dots$ ,  $[\mathbf{S}_{\overline{\gamma}}^{[N-2, 2]}]_{N-2, N}$ .

From Eq. (41), the symmetry coordinate  $[\mathbf{S}_{\overline{\gamma}}^{[N-2, 2]}]_{ij}$  only involves motions of the first  $j$  particles (Note  $i \leq j-2$ , and for the particle labels  $m, n > j$  the Heaviside and Kronecker delta functions are zero). Thus, the complexity of the functional form of  $[\mathbf{S}_{\overline{\gamma}}^{[N-2, 2]}]_{ij}$  and the motions it describes builds up slowly and systematically as more particles are added to the system. The symmetry coordinate,  $[\mathbf{S}_{\overline{\gamma}}^{[N-2, 2]}]_{14}$ , involves the motion of only the first four particles with the simultaneous opening of two interparticle angles  $\theta_{13}$  and  $\theta_{24}$ , and closing of two different interparticle angles,  $\theta_{14}$  and  $\theta_{23}$ . (cf. the  $E$  mode of methane. Note that there are no  $[N-2, 2]$  modes when  $N$  drops below four.) For this lowest value of  $N$ , the positive and negative angular displacements have equal values, however as  $N$  increases, this collective motion quickly evolves to create a compressional motion with a single dominant angle opening and closing while the other interparticle angles that number  $N(N-1)/2-1$  make small adjustments. (See Section V A for a more detailed discussion.)

#### IV. MOTIONS ASSOCIATED WITH THE NORMAL MODES

From Eq. (29) shown again below, the symmetry coordinates in the  $[N]$  and  $[N-1, 1]$  sectors are mixed to form a normal coordinate.

$$\begin{aligned} \mathbf{q}'_{\pm}^{[N]} &= c_{\pm}^{[N]} \left( \cos \theta_{\pm}^{[N]} [\mathbf{S}_{\overline{\gamma}}^{[N]}] + \sin \theta_{\pm}^{[N]} [\mathbf{S}_{\overline{\gamma}}^{[N]}] \right) \\ \mathbf{q}'_{\xi\pm}^{[N-1, 1]} &= c_{\pm}^{[N-1, 1]} \left( \cos \theta_{\pm}^{[N-1, 1]} [\mathbf{S}_{\overline{\gamma}}^{[N-1, 1]}]_{\xi} \right. \\ &\quad \left. + \sin \theta_{\pm}^{[N-1, 1]} [\mathbf{S}_{\overline{\gamma}}^{[N-1, 1]}]_{\xi} \right) \end{aligned} \quad (42)$$

where  $1 \leq \xi \leq N-1$ . Thus, depending on the value of the mixing angles, the normal modes, which are the solutions at first order of the Schrödinger equation will be a mixture of radial and angular behavior for the  $[N]$  and  $[N-1, 1]$  sectors. The  $[N-2, 2]$  sector has only angular behavior as noted above and so does not mix with other symmetry coordinates. The value of the mixing angles, of course, depends on the Hamiltonian terms at this first perturbation order. Choosing various confining and interparticle potentials will result in different values for the mixing coefficients and different collective motion as dictated by the Hamiltonian.

#### V. COLLECTIVE BEHAVIOR AS A FUNCTION OF $N$

In this section, I consider the evolution of behavior of the symmetry coordinates and then the normal coordinates as a function of the number of particles,  $N$ . For low values of  $N$  it is possible to find molecular equivalents to characterize the behavior of the symmetry coordinates. (These comparisons are of course only approximate since the molecular systems have Hamiltonians with the hetero atom providing Coulombic confinement.) For the  $[N]$  radial and angular modes, the  $A_1$  modes of ammonia,  $NH_3$  with their symmetric breathing and bending motions are good equivalents. The radial and angular  $[N-1, 1]$  modes are similar to the two  $E$  ammonia modes for small  $N$ . These motions show one of the hydrogen atoms moving out of sync with the other two hydrogens, thus described as asymmetric stretching and asymmetric bending modes. The  $[N-2, 2]$  modes need to have at least four atoms in addition to the center atom of the molecule. Methane,  $CH_4$  has a purely angular mode in an  $E$  mode of this molecule in which the bonds to the hydrogen atoms show bending motions that alternately open and close interparticle angles. These motions can be viewed at the following links: [www.chemtube3d.com/vibrationsnh3/](http://www.chemtube3d.com/vibrationsnh3/) and [www.chemtube3d.com/vibrationsch4/](http://www.chemtube3d.com/vibrationsch4/)

As  $N$  increases, these motions evolve in several ways. There are in fact three ways that an increase in  $N$  can affect the character of the normal modes.

A) As noted above in Section III a.- e., the analytic forms of the particle motion have explicit  $N$  or  $\xi$  ( $1 \leq \xi \leq N-1$ ) or  $i, j$  dependence ( $1 \leq i \leq j-2$ ,  $4 \leq j \leq N$ ) (See Eqs. (36, 38 - 41) that can affect the character of the motion of particles contributing to a particular symmetry coordinate and thus the normal coordinates. As more particles are added to the system, the behavior of these larger systems can become qualitatively quite different from few particle systems with low values of  $N$ , e.g.  $3 \leq N \leq 6$ .

B) Second, the amount of mixing of the radial and angular symmetry coordinates in the  $[N]$  and  $[N-1, 1]$  sectors (i.e. the values of  $\cos \theta_{\pm}^{[N]}$ ,  $\sin \theta_{\pm}^{[N]}$ ,  $\cos \theta_{\pm}^{[N-1, 1]}$  and  $\sin \theta_{\pm}^{[N-1, 1]}$  in Eq. (42)) can evolve as  $N$  increases.

C) And finally, the frequency of vibration of the normal modes can change as a function of  $N$ .

Although general observations can be made, all three of these effects ultimately depend on the particular Hamiltonian of the system. As a specific example, I will look at these effects using a recently studied Hamiltonian for a system of identical fermions in the unitary regime.

##### A. Explicit $N$ dependence

In the analytic expressions for the particle motions contributing to the symmetry coordinates, Eqs. (36, 38 - 41),

there is some explicit  $N$  dependence that affects the behavior as  $N$  increases.

**The  $[N]$  sector.** For the symmetric stretch motion in the  $[N]$  sector, the character of this breathing motion remains the same as  $N$  increases with the radial displacements decreasing as  $N$  increases. The particles move along their individual radii out and then in toward the center of the trap, keeping their interparticle angles constant as they oscillate about the zeroth order configuration.

For the angular motion in the  $[N]$  sector, the symmetric bend motion of the interparticle angles for small  $N$ , (cf. the  $A_1$  mode of ammonia) evolves into a center of mass motion as  $N$  increases. The particles undergo identical angular displacements that decrease in size as  $N$  increases resulting in motion where the whole ensemble "jiggles" in response to an excitation of the center of mass mode. These jiggles are caused by the particles moving past the trap center and then back keeping their radii constant while changing their interparticle angles compared to the zeroth order configuration. As expected, the frequency of this mode, as shown in Section VC, cleanly separates out for all values of  $N$  at exactly twice the trap frequency (The atoms move past the trap center twice in one cycle.), reflecting the fact the center of mass motion is independent of particle interactions.

For the  $[N-1, 1]$  and  $[N-2, 2]$  sectors, the analytic forms of the  $(r_\xi^{[N-1, 1]})_i$ ,  $(\gamma_\xi^{[N-1, 1]})_{ij}$  and  $(\gamma_{ij}^{[N-2, 2]})_{mn}$  contain parameters associated with  $N$  that change the character of the motion as  $N$  changes.

**The  $[N-1, 1]$  sector.** As discussed above, in the  $[N-1, 1]$  sector, the appearance of  $\xi$  in the last terms of Eqs. (39) and (40) weights the response of the  $\xi + 1$ st particle. For small values of  $N$  and thus small  $\xi$  ( $1 \leq \xi \leq N-1$ ), the motion of this last  $\xi + 1$ st particle, which has opposite direction to the first  $\xi$  particles, appears as a simple asymmetric stretch or bend. As  $N$  becomes large, and thus  $\xi$  can also approach large values, this motion acquires such a large displacement compared to the remaining particles that it is more appropriately characterized as a particle-hole excitation due to single particle radial or angular motion away from the other particles ( $\xi$  in number) participating in this collective motion. This change in character from asymmetric stretch (or bend) to single particle radial (or angular) excitation happens quite quickly as  $N$  and  $\xi$  increase with e.g.  $N = 10$  and  $\xi = N-1 = 9$  showing obvious single particle behavior as the  $\xi + 1^{st} = 10^{th}$  particle moves with a radial displacement nine times larger than the other  $\xi$  particles and in the opposite direction. Note that the displacements of all  $\xi + 1$  particles sum to zero (1 (particle)  $\times$  a displacement of  $\xi = \xi$  particles  $\times$  a displacement of 1) reflecting the fact that this motion is a rearrangement of

the particles within the ensemble creating a hole, not the loss of a particle due to radial or angular motion.

**The  $[N-2, 2]$  sector.** In the  $[N-2, 2]$  sector which has totally angular behavior, a similar evolution of character is observed as  $N$  increases. Consider the symmetry coordinate  $[S_{\gamma'}^{[N-2, 2]}]_{ij}$  where ( $1 \leq i \leq j-2$ ,  $4 \leq j \leq N$ ), and let  $i$  and  $j$  assume their highest values,  $i = N-2$  and  $j = N$  so all  $N$  particles will be involved in the motion of this symmetry coordinate  $[S_{\gamma'}^{[N-2, 2]}]_{N-2, N}$ . Examining each of the  $N(N-1)/2$  angular displacements,  $(\gamma_{ij}^{[N-2, 2]})_{mn}$ , for particles  $m, n$  ( $1 \leq m < n \leq N$ ) that contribute to the corresponding total angle cosines,  $(\gamma_{ij}^{[N-2, 2]})_{mn} = \gamma_\infty + \delta^{\frac{1}{2}}(\gamma_{ij}^{[N-2, 2]})_{mn}$ , it is clear from Eq. 41 that there are 3 different magnitudes of  $\gamma'$  appearing for three types of interparticle angles. The displacement  $(\gamma_{ij}^{[N-2, 2]})_{mn}$  is the first-order correction in  $\delta = 1/D$  to the total angle cosine allowing a determination of the value of the interparticle angle,  $(\gamma_{ij}^{[N-2, 2]})_{mn} = \cos \theta_{mn}$ . Then  $\theta_{mn} - \theta_\infty$  gives the displacement. To determine  $\theta_\infty = \arccos \gamma_\infty$  and thus the displacement, a specific Hamiltonian must be chosen.

*a. The dominant interparticle angle.* When the  $m^{th}$  and  $n^{th}$  particles assume the values,  $m = i+1 = N-1$  and  $n = j = N$ , the weighting factors  $i\delta_{i+1, m}$  and  $(j-3)\delta_{j, n}$  in Eq. 41 multiply together producing a large positive factor of  $i(j-3) = (N-2)(N-3)$  in the displacement contribution to the angle cosines,  $(\gamma_{ij}^{[N-2, 2]})_{mn} = (\gamma_{N-2, N}^{[N-2, 2]})_{N-1, N}$ .

*b. Nearest neighbor interparticle angles.* For  $(\gamma_{ij}^{[N-2, 2]})_{mn}$  which have either  $m = i+1 = N-1$  or  $n = j = N$ , (but not both) one or the other weighting factor in Eq. 41 contributes resulting in a negative factor of  $-(N-3)$  in the expression for the displacement. These  $(\gamma_{ij}^{[N-2, 2]})_{mn}$  are associated with angles  $\theta_{mn}$  that are nearest neighbor interparticle angles with the dominant angle  $\theta_{N-1, N}$  discussed in part *a.* above. Thus these interparticle angles are responding to the motion of this dominant angle. If the dominant angle is opening, these neighboring angles are compressing and vice versa. These angles are:  $\gamma'_{1, N}, \gamma'_{2, N}, \gamma'_{3, N}, \gamma'_{4, N}, \dots, \gamma'_{N-2, N}$  and  $\gamma'_{1, N-1}, \gamma'_{2, N-1}, \gamma'_{3, N-1}, \gamma'_{4, N-1}, \dots, \gamma'_{N-2, N-1}$  numbering  $2(N-2)$ . (I have dropped the indices  $i, j$  referencing the particular symmetry coordinate.)

*c. Third type of interparticle angle.* This leaves  $N(N-1)/2 - 2(N-2) - 1$  interparticle angles which have a third type of displacement for  $(\gamma_{ij}^{[N-2, 2]})_{mn}$  which includes a small factor of  $+2$  since neither weighting factor in Eq. 41 contributes.

All the displacements for the particles  $m, n$  contributing to the motion of the  $i, j^{th}$  symmetry coordinate include an identical factor of  $[S_{\gamma'}^{[N-2, 2]}]_{i, j}$  as well as a normalization factor of  $\frac{1}{\sqrt{i(i+1)(j-3)(j-2)}}$ .

Note also that all the displacements sum to zero:  $1 \times (N-2)(N-3) - 2(N-2) \times (N-3) + (N(N-1)/2 - 2(N-2) - 1) \times 2 \equiv 0$ , reflecting the fact that the particles are simply rearranging their positions within the confined angular space they occupy.

For very low values of  $N$ , these expressions yield behavior that is qualitatively analogous to the normal mode behavior seen in few-body molecular systems like ammonia or methane. For example, for  $N = 4$ , there is one dominant interparticle angle, four nearest neighbor interparticle angles,  $2(N-2) = 4$ , and a single interparticle angle of the third type,  $N(N-1)/2 - 2(N-2) - 1 = 1$ . The displacements of the dominant angle and the single angle of the third type are equal for this lowest value of  $N$  (the factor  $(N-2)(N-3) = 2$  for  $N = 4$ ) while the four nearest neighbor angles have a smaller displacement (with a factor of  $N-3 = 1$ ) similar to the behavior of an E mode of methane.

As  $N$  increases, the relative numbers of the three different interparticle angles change quickly with the third type of interparticle angle, which is not a nearest neighbor of the dominant angle and thus has a small response, quickly becoming the overwhelmingly largest number of interparticle angles. The first type always has a single dominant angle with the largest correction to the maximally symmetric zeroth-order configuration. The second type, which has a noticeable response to the opening or closing of the dominant angle, has  $2(N-2)$  angles, a number that increases linearly with  $N$ , while the third type of angle which has a negligible response for  $N \gg 1$  has  $N(N-1)/2 - 2(N-2) - 1$  interparticle angles which increases as  $N^2/2$ , quickly becoming the greatest part of an ensemble of  $N$  particles that is undergoing this collective motion. For example, for  $N = 10$  with  $N(N-1)/2 = 45$  interparticle angles, there is a single dominant angle, 16 angles that are nearest neighbors and 28 angles with a very small response in the third group. For  $N = 100$ , there are 4950 interparticle angles: one dominant angle, 196 nearest neighbor angles that show a noticeable response and 4753 angles that have a very small response.

Thus a picture emerges as  $N$  increases of compressional or phonon behavior for the motion in this  $[N-2, 2]$  sector. These  $[N-2, 2]$  modes involve oscillations in the angles that push the atoms together and pull them apart with no change in the particles' radial positions. This type of motion is best characterized as a compressional stationary wave i.e. a phonon oscillation. This is consistent with the very low frequency of this mode compared to the frequencies of the other four types of normal coordinates as will be shown in Section V C and the large zero-point energy as seen in Eq. (15).

**Examples.** The three types of interparticle angles have *displacement* values that also depend on the value of  $N$ , evolving from displacements that are roughly comparable for all three types of angles for low values of  $N$ , e.g.  $4 \leq N \leq 6$  to displacements that are quite different

in magnitude differing by factors  $\sim N$  and  $\sim N^2$  as  $N$  increases. Using the ratios of the different factors discussed above in the expressions for the angular displacements, the dominant angle has an angular displacement value of  $(N-2)(N-3)$  that is a factor of  $N-2$  times larger than the angular displacements of  $-(N-3)$  of the nearest neighbor angles and is a factor of  $(N-2)(N-3)/2$  times larger than the angular displacements of 2 for the third type of interparticle angle. As explicit examples, I will look at the ratios of the three types of displacements for two values of  $N$ :  $N = 4$  and  $N = 10$  and will again consider the motion of individual particles participating in the collective motion of the symmetry coordinate  $[S_{\vec{\gamma}}^{[N-2, 2]}]_{ij}$  which has the highest values of  $i$  and  $j$  ( $i = N-2, j = N$ ) and thus involves the motion of all  $N$  particles. For  $N = 4$ , the symmetry coordinate is expected to have behavior similar to an E mode of methane; and for  $N = 10$ , it will be seen that the behavior of this symmetry coordinate in the  $[N-2, 2]$  sector has already evolved into compressional behavior.

For the lowest value of  $N = 4$ , the displacement of the dominant angle is twice (the factor  $N-2 = 2$ ) the displacement of the nearest neighbor angles and equal to the displacement (with factor  $(N-2)(N-3)/2 = 1$ ) of the single angle in the third type. Thus, the dominant angle and the single angle of the third type have a contribution to the angle cosine that is twice as large as the four nearest neighbor angles. The interparticle angle  $\theta_{12}$  associated with particles 1 and 2 opens and closes by the same amount and in sync with the dominant angle  $\theta_{34}$  between particles 3 and 4. The nearest neighbor angles,  $\theta_{13}, \theta_{14}, \theta_{23}, \theta_{24}$ , open (and then close) by an amount that is roughly half as large in response to the closing (opening) of the dominant angle. (Since the value of  $\gamma_\infty$  is typically close to zero which is the value for mean field interactions, the angular displacements to the angle cosines roughly give the actual angles of these motions.)

Thus, the four particles involved in the collective motion of the symmetry coordinate  $[S_{\vec{\gamma}}^{[N-2, 2]}]_{24}$  perform a simultaneous opening and closing of two different interparticle angles,  $\theta_{34}$  and  $\theta_{12}$  similar to an E mode of methane with the neighboring angles making smaller adjustments.

A similar analysis for the case of  $N = 10$  shows clearly that the motion of the particles participating in this symmetry coordinate has evolved from the methane picture of two interparticle angles opening and closing in sync, to behavior that looks much more like a compressional wave. For  $N = 10$  and letting  $i$  and  $j$  assume their largest values,  $i = 8, j = 10$ , I analyze the behavior of the particles participating in the symmetry coordinate  $[S_{\vec{\gamma}}^{[N-2, 2]}]_{8,10}$ . The dominant interparticle angle  $\theta_{9,10}$  closes (and then opens) with an angular displacement that is eight times (the factor  $N-2 = 8$ ) the angular displacement of the 16 nearest neighbor angles and 28 times (the factor  $(N-2)(N-3)/2 = 28$ ) the angular dis-

placement of the 28 interparticle angles of the third type. Thus both the nearest neighbor angles and especially the third type of interparticle angle which has become the largest group have already begun to have a very small response compared to the change in the dominant angle.

This trend is expected to continue as  $N$  increases and the number of interparticle angles in the third type becomes very large. (For  $N = 100$ , the dominant angle closes by an angular displacement that is 98 times (the factor  $N - 2 = 98$ ) larger than the 196 nearest neighbor angles which by open a very small amount, while the 4753 interparticle angles of the third type adjust by an even smaller amount, 4753 times (the factor  $(N - 2)(N - 3)/2 = 98 \times 97/2 = 4753$ ) smaller than the dominant angle, more than three orders of magnitude smaller, clearly a negligible response.

### B. Mixing coefficients as a function of $N$

For the mixing coefficients that determine the radial/angular mixing in the normal modes for the  $[N]$  and

$[N - 1, 1]$  sectors, very few general comments can be made without specifying a particular Hamiltonian. The mixing coefficients as defined in Eq. (32) have a complicated  $N$  dependence that originates in the Hamiltonian terms at first order. All the terms in the Hamiltonian have explicit  $N$  dependence which affects the mixing of the radial and angular modes of the  $[N]$  and  $[N - 1, 1]$  sectors. In particular, the type of confining potential and the particular interparticle interaction chosen will affect the  $N$  dependence of the normal modes' behavior. (Of course, the type of confining potential and interparticle interaction potential have effects on the character of the normal modes through the mixing coefficients (as well as the frequencies) apart from the  $N$  dependence that I am studying in this paper.)

In the case of the recently studied system of identical fermions in the unitary regime which has been intensely studied in the laboratory, the mixing coefficients for the  $[N]$  sector have the following form:

$$\cos\theta_+^{[N]} = \frac{\sqrt{2}\sqrt{N-1}(c + (N/2 - 1)d)}{\sqrt{2(N-1)(c + (N/2 - 1)d)^2 + (-a - (N-1)b + \lambda_{[N]}^+)^2}} \quad (43)$$

$$\sin\theta_+^{[N]} = \frac{-a - (N-1)b + \lambda_{[N]}^+}{\sqrt{2(N-1)(c + (N/2 - 1)d)^2 + (-a - (N-1)b + \lambda_{[N]}^+)^2}} \quad (44)$$

$$\cos\theta_-^{[N]} = \frac{\sqrt{2}\sqrt{N-1}(c + (N/2 - 1)d)}{\sqrt{2(N-1)(c + (N/2 - 1)d)^2 + (-a - (N-1)b + \lambda_{[N]}^-)^2}} \quad (45)$$

$$\sin\theta_-^{[N]} = \frac{-a - (N-1)b + \lambda_{[N]}^-}{\sqrt{2(N-1)(c + (N/2 - 1)d)^2 + (-a - (N-1)b + \lambda_{[N]}^-)^2}} \quad (46)$$

where  $\lambda_{[N]}^\pm$  is given by Eq. 27. The quantities  $a, b, c, d$ , and  $\lambda_{[N]}^\pm$ , are defined in Eq.(42) in Ref. [22] in terms of the  $F$  and  $G$  elements and have explicit  $N$  dependence as well as  $N$  dependence from the  $F$  and  $G$  elements of Eq. 12 from the specific Hamiltonian. These  $F$  and  $G$  elements are defined in Ref. [22] for three different Hamiltonians in Eqs. (75, 76, 100, 101, 119, 120) and exhibit explicit  $N$  dependence that originates in the Hamiltonian terms at first order. Thus there are three layers of analytic expressions that can bring in  $N$  dependence: the expressions for  $\cos\theta_\pm^{[N]}$  and  $\sin\theta_\pm^{[N]}$  in Eqs. (43-46) above, the expressions for  $a, b, c, d$ , and  $\lambda_{[N]}^\pm$  and the expressions for the  $F$  and  $G$  elements for a specific Hamiltonian.

I show the resulting behavior of the mixing coefficients as a function of  $N$  for a system of identical fermions in

the unitary regime in Figs. (1-4). In Fig. 1, I have plotted the square of the mixing coefficients,  $|\cos\theta_+^{[N]}|^2$  and  $|\sin\theta_+^{[N]}|^2$  for  $q_+^{[N]}$ :

$$q_+^{[N]} = c_+^{[N]} \left( \cos\theta_+^{[N]} [\mathbf{S}_{\hat{r}'}^{[N]}] + \sin\theta_+^{[N]} [\mathbf{S}_{\hat{\varphi}'}^{[N]}] \right)$$

as a function of  $N$ . The square of these coefficients gives the probability associated with each symmetry coordinate,  $[\mathbf{S}_{\hat{r}'}^{[N]}]$  or  $[\mathbf{S}_{\hat{\varphi}'}^{[N]}]$ , in the expression for the normal mode,  $q_+^{[N]}$ . The plot shows that the character of the normal mode  $q_+^{[N]}$  is almost purely angular for  $N \lesssim 30$  after which there is a gradual crossing of character between  $N = 30$  and  $N = 200$  when the normal mode has mixed radial and angular character. For  $N \geq 200$  the

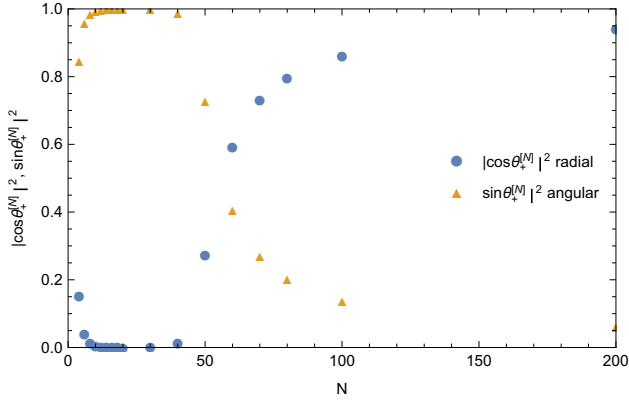


FIG. 1: The square of the mixing coefficients  $|\cos \theta_+^{[N]}|^2$  and  $|\sin \theta_+^{[N]}|^2$  for the normal mode  $q_+^{[N]}$  as a function of  $N$ .

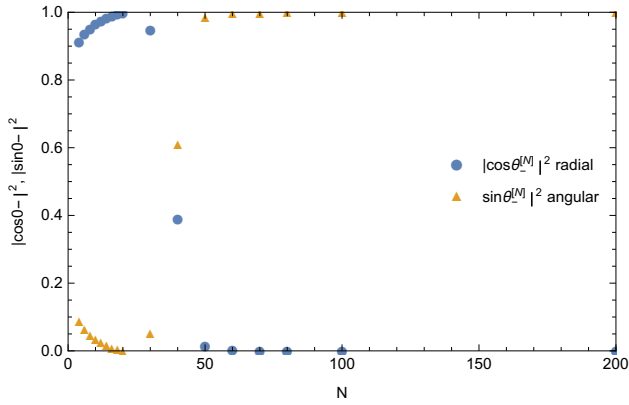


FIG. 2: The square of the mixing coefficients  $|\cos \theta_-^{[N]}|^2$  and  $|\sin \theta_-^{[N]}|^2$  for the normal mode  $q_-^{[N]}$  as a function of  $N$ .

character is  $> 90\%$  radial and for  $N \gg 1$ , the character becomes almost purely radial.

The other normal mode in the  $[N]$  sector,  $q_-^{[N]}$  has complementary behavior, starting out totally radial and switching to totally angular as shown in Fig. 2. In this case, the crossover is quite sharp, starting again around  $N \sim 30$ , but finishing the crossover by  $N = 50$ . So this normal mode,  $q_-^{[N]}$ , is purely radial for low  $N$  and purely angular for very large values of  $N$ . It has mixed radial/angular character for a very small range of  $N$ .

A bit of inspection reveals that this behavior is being dictated to a large extent by the explicit  $N$  dependence in the expressions for  $\cos \theta_{\pm}^{[N]}$  and  $\sin \theta_{\pm}^{[N]}$  (Eqs. (43-46) above) which have alternating limits of 0 or 1 as  $N \rightarrow 1$  or  $N \rightarrow \infty$ . The position and shape of the crossover is influenced by the other sources of  $N$  dependence that originate in the specific Hamiltonian.

The mixing coefficients for the  $[N-1, 1]$  sector have the following form:

$$\cos \theta_+^{[N-1,1]} = \frac{\sqrt{N-2}(c-d)}{\sqrt{(N-2)(c-d)^2 + (-a+b+\lambda_{[N-1,1]}^+)^2}} \quad (47)$$

$$\sin \theta_+^{[N-1,1]} = \frac{-a+b+\lambda_{[N-1,1]}^+}{\sqrt{(N-2)(c-d)^2 + (-a+b+\lambda_{[N-1,1]}^+)^2}} \quad (48)$$

$$\cos \theta_-^{[N-1,1]} = \frac{\sqrt{N-2}(c-d)}{\sqrt{(N-2)(c-d)^2 + (-a+b+\lambda_{[N-1,1]}^-)^2}} \quad (49)$$

$$\sin \theta_-^{[N-1,1]} = \frac{-a+b+\lambda_{[N-1,1]}^-}{\sqrt{(N-2)(c-d)^2 + (-a+b+\lambda_{[N-1,1]}^-)^2}} \quad (50)$$

where the quantities  $a, b, c, d$ , and  $\lambda_{[N-1,1]}^{\pm}$ , as well as the  $F$  and  $G$  elements are defined as before.

In Fig. 3, I have plotted the square of the mixing coefficients for  $q_{\xi+}^{[N-1,1]}$ , again for a Hamiltonian describing

a system of identical fermions in the unitary regime. The plot shows that the character of the normal mode  $q_{\xi+}^{[N-1,1]}$  is almost purely angular for  $N \lesssim 10$  after which there is a rather sudden crossing of character and then a gradual trend toward purely radial character. For

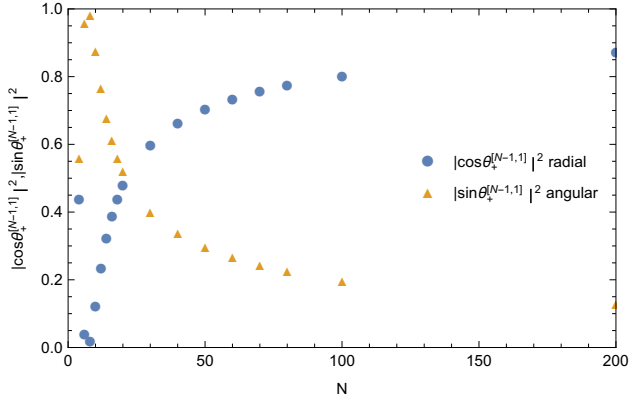


FIG. 3: The square of the mixing coefficients  $|\cos \theta_+^{[N-1,1]}|^2$  and  $|\sin \theta_+^{[N-1,1]}|^2$  for the normal mode  $q_+^{[N-1,1]}$  as a function of  $N$ .

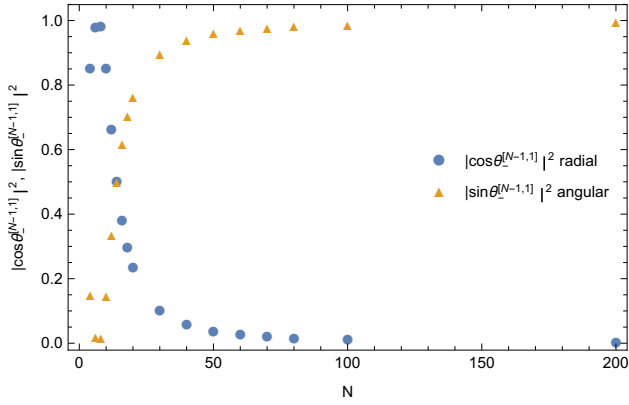


FIG. 4: The square of the mixing coefficients  $|\cos \theta_-^{[N-1,1]}|^2$  and  $|\sin \theta_-^{[N-1,1]}|^2$  for the normal mode  $q_-^{[N-1,1]}$  as a function of  $N$ .

$N \gg 1$ , the character is almost purely radial. The other normal mode in the  $[N-1, 1]$  sector,  $q_-^{[N-1,1]}$  has complementary behavior, starting out totally radial and switching to totally angular as shown in Fig. 4. In this case the crossing is quite sharp.

Analogous to the  $[N]$  sector, this behavior is being dictated to a large extent by the explicit  $N$  dependence in the expressions for  $\cos \theta_\pm^{[N-1,1]}$  and  $\sin \theta_\pm^{[N-1,1]}$  in Eqs. (47-50) above which have alternating limits of 0 or 1 as  $N \rightarrow 2$  or  $N \rightarrow \infty$ . The position and shape of the crossover is influenced by the other sources of  $N$  dependence that originate in the specific Hamiltonian.

### C. Normal mode frequencies as a function of $N$ .

Analytic expressions for the normal mode frequencies were derived in Ref. [22] using a method outlined in Appendices B and C of that paper which derives analytic formulas for the roots,  $\lambda_\mu$ , of the  $FG$  secular equation. The normal-mode vibrational frequencies,  $\bar{\omega}_\mu^2$ , are related

to the roots  $\lambda_\mu$  of **FG** by:

$$\lambda_\mu = \bar{\omega}_\mu^2, \quad (51)$$

The two frequencies associated with the  $\lambda_0$  roots of multiplicity one are of the form

$$\bar{\omega}_{0\pm} = \sqrt{\eta_0 \pm \sqrt{\eta_0^2 - \Delta_0}}, \quad (52)$$

where:

$$\begin{aligned} \eta_0 = \frac{1}{2} & \left[ a - (N-1)b + g + 2(N-2)h \right. \\ & \left. + \frac{(N-2)(N-3)}{2} \iota \right] \\ \Delta_0 = (a - (N-1)b) & \left[ g + 2(N-2)h - \frac{(N-2)(N-3)}{2} \iota \right] \\ & - \frac{N-2}{2} (2c + (N-2)d)(2e + (N-2)f). \end{aligned} \quad (53)$$

For the two  $N-1$  multiplicity roots, the frequencies are of the form

$$\bar{\omega}_{1\pm} = \sqrt{\eta_1 \pm \sqrt{\eta_1^2 - \Delta_1}}, \quad (54)$$

where  $\eta_1$  and  $\Delta_1$  are given by:

$$\begin{aligned} \eta_1 &= \frac{1}{2} [a - b + g + (N-4)h - (N-3)\iota] \\ \Delta_1 &= (N-2)(c-d)(e-f) + (a-b) \\ &\quad \times [g + (N-4)h - (N-3)\iota]. \end{aligned} \quad (55)$$

The frequency  $\bar{\omega}_2$ , associated with the root  $\lambda_2$  of multiplicity  $N(N-3)/2$  is given by:

$$\bar{\omega}_2 = \sqrt{g - 2h + \iota}. \quad (56)$$

The quantities  $a, b, c, d, e, f, g, h, i$  are defined as before in Eq. (42) in Ref [22] in terms of the  $F$  and  $G$  elements and have explicit  $N$  dependence as well as  $N$  dependence from the  $F$  and  $G$  elements from a particular Hamiltonian.

Thus the analytic expressions for the frequencies (like the mixing coefficients) have three layers of  $N$  dependence: explicit  $N$  dependence in the formulas for  $\eta_0, \Delta_0, \eta_1$  and  $\Delta_1$  in Eqs (53) and (55); explicit  $N$  dependence in the formulas for the quantities  $a, b, c, d, e, f, g, h, i$ , and finally the  $N$  dependence in the  $F$  and  $G$  elements from a specific Hamiltonian in these formulas.

In Figs. (5)-(7), I show the  $N$  dependence of the frequencies for the five types of normal modes for a Hamiltonian of an ensemble of identical fermions in the unitary regime.

In Fig. (5), the frequencies  $\bar{\omega}_{0+}$  and  $\bar{\omega}_{0-}$  in the  $[N]$  sector show a clear avoided crossing as the characters of the normal modes  $q_+^{[N]}$  and  $q_-^{[N]}$  change from angular to

radial for  $q_+^{[N]}$  and radial to angular for  $q_-^{[N]}$ . The radial behavior is associated with a frequency that starts below the center of mass frequency for low  $N$  and then rises above the center of mass frequency as  $N$  increases. Note that the angular behavior is associated with a frequency that is exactly twice the trap frequency for all values of  $N$  revealing the separation of a center of mass coordinate. As analyzed in Section III, this angular motion in the  $[N]$  sector looks like a symmetric bending motion for small values of  $N$  as seen in the  $A_1$  mode of ammonia, but evolves into a rigid center of mass movement of the whole ensemble with the radial interparticle distances remaining rigidly constant as the entire ensemble moves relative to the center of the trap creating small displacements for the interparticle angles.

In Fig. (6), the frequencies  $\bar{\omega}_{1+}$  and  $\bar{\omega}_{1-}$  in the  $[N-1, 1]$  sector show behavior that starts out with both frequencies  $\sim 1.3$  times the trap frequency for low values of  $N$ . As  $N$  increases these two frequencies rapidly separate, one,  $\bar{\omega}_{1-}$ , associated with angular behavior, going to the trap frequency and the other,  $\bar{\omega}_{1+}$ , describing radial behavior, increasing slowly. In both these sectors,  $[N]$  and  $[N-1, 1]$ , the radial frequency is higher than the corresponding angular frequency which is expected and is also seen for the small molecules like ammonia and methane that offer good molecular equivalents.

In Fig. (7), the frequency  $\bar{\omega}_2$  of the  $[N-2, 2]$  sector shows behavior that starts out for low values of  $N$  at values near the trap frequency. As  $N$  increases this frequency rapidly decreases to extremely small values, several orders of magnitude smaller than the trap frequency consistent with the slow oscillations of a phonon mode.

Inspection of the sources of  $N$  dependence reveal that the frequencies shown in Figs. (5)-(7), for a Hamiltonian of identical fermions in the unitary regime show a complicated dependence on all three layers of  $N$  dependence. This result differs from the behavior of the mixing coefficients for the same Hamiltonian which showed behavior as a function of  $N$  that was dominated by the explicit  $N$  dependence in Eqs. (43-46) and Eqs. (47-50) and was not as sensitive to the other sources of  $N$  from the specific Hamiltonian.

## VI. SUMMARY AND FINAL THOUGHTS

In this study, I have looked in detail at both the macroscopic collective behavior and the microscopic contributions of individual particles to this behavior for the normal mode solutions to the symmetry-invariant perturbation first order equation in inverse dimensionality for a system of confined, interacting identical particles. These normal mode solutions were previously obtained analytically as a function of  $N$  and used to obtain accurate results for energies, frequencies, wave functions, and density profiles for systems of identical bosons [23, 24, 28, 29] and energies, frequencies[30] and thermodynamic quantities[19] for ultracold fermions in the

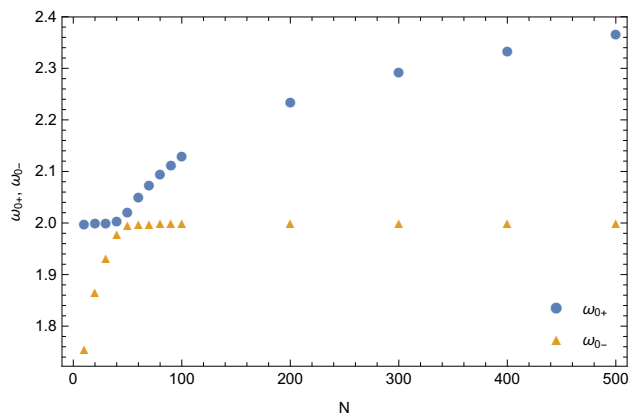


FIG. 5: The frequencies  $\bar{\omega}_{0\pm}$  in units of the trap frequency for the normal modes  $q_{\pm}^{[N]}$  as a function of  $N$ .

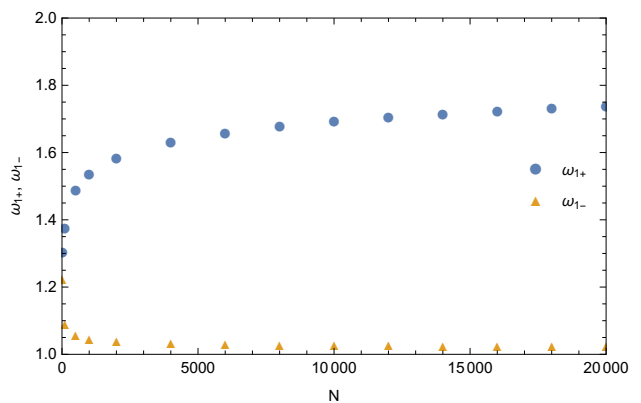


FIG. 6: The frequencies  $\bar{\omega}_{1\pm}$  in units of the trap frequency for the normal modes  $q_{\pm}^{[N-1,1]}$  as a function of  $N$ .

unitary regime.

These solutions have been tested against an exactly solvable model problem of harmonically interacting particles under harmonic confinement[23]. Comparing this wave function to the exact analytic wave function obtained in an independent solution, exact agreement was found (to ten or more digits of accuracy), confirming this general theory for a fully interacting  $N$ -body system in three dimensions[23] and verifying the analytic expressions for this normal mode basis. We also tested this general, fully interacting wave function for bosons of Ref. [21], exact through first order, by deriving a property, the density profile of the ground state, for the same model problem. Our density profile is indistinguishable from the  $D = 3$  first-order result from the independent solution of this fully interacting,  $N$ -body problem[24].

These earlier studies verifying the general formalism, did not focus on the physical character of this symmetry basis used to obtain the normal modes solutions. As mentioned earlier, our construction of the symmetry coordinates was done systematically as described in Ref. [21] so the symmetry coordinates which transform irreducibly under  $S_N$  have the simplest functional forms



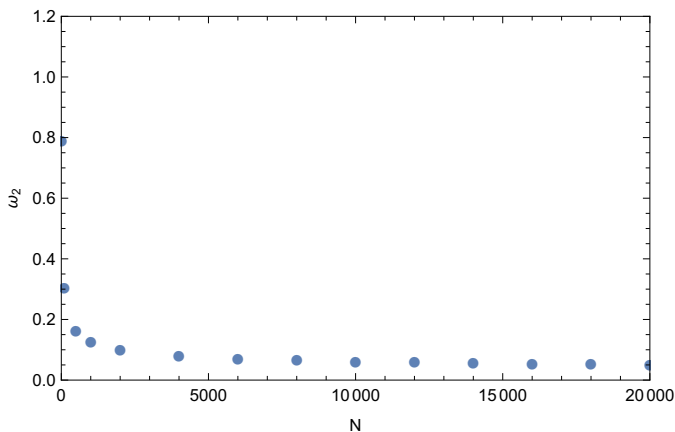


FIG. 7: The frequency  $\bar{\omega}_2$  in units of the trap frequency for the normal mode  $q'^{[N-2,2]}$  as a function of  $N$ .

possible. The first symmetry coordinate involves only two of the particles and each succeeding symmetry coordinate was chosen to have the next simplest functional form possible under the requirement that it transforms irreducibly under  $S_N$  etc. With this choice the complexity of the motions described by the symmetry coordinates was kept to a minimum, building up incrementally as additional particles were involved in the motion, ensuring that there was no disruption of lower  $N$  symmetry coordinates. This process was chosen primarily to simplify the mathematical complexity of this basis. Other choices would have resulted in different mathematical functions that still comprised a basis for the normal mode solutions in each sector. Note that the symmetry coordinates depend only on the symmetry structure of the Hamiltonian, not on specific details of the interparticle potential, unlike the normal mode coordinates which depend on the specific details of the potentials involved.

Our initial studies using these symmetry coordinates were focused on ground states of systems of ultracold bosons[28, 29] and later fermions[30] The first use of excited states using this many-body formalism was in a recent paper studying thermodynamic quantities for identical fermions in the unitary regime. Constructing the partition function in this study required the use of a large number of excited states from the normal mode spectrum (which has an infinite number of equally spaced states). These states are chosen specifically to comply with the enforcement of the Pauli principle, thus connecting the Pauli principle to many-body interaction dynamics through the normal modes. The success of this study in obtaining thermodynamic quantities for the energy, entropy and heat capacity that agree quite well with experimental data has increased the interest in investigating the physical character of these states since they offer the possibility of acquiring physical intuition into the dynamics of the collective motion supported by this unitary regime. In particular, the phonon character of the normal modes with the lowest frequency and the ra-

dial (or angular) excitation of a single particle out of this mode, i.e. a particle-hole excitation, present a picture of the dynamics that leads to a gapped spectrum and collective behavior in the form of superfluidity. With this motivation, I have investigated closely both the macroscopic behavior of each of the five types of normal modes and the microscopic contributions of each particle to this collective behavior, studying the evolution of collective motion as the number of particles increases.

**Summary.** In summary, my analysis has shown a consistent picture of behavior evolving smoothly and rapidly from the low  $N$  systems that have good molecular equivalents, as seen in the behavior of ammonia and methane to very different character for the collective motion of larger  $N$  systems. A number of observations have been made from this analysis that may prove useful in understanding the contribution of particle behavior to the emerging collective behavior of an ensemble. I list them below:

1) The analytic expressions for the normal modes produce behavior for small  $N$  that is analogous to the known behavior of small molecular systems such as ammonia and methane whose atoms move under Coulombic confinement.

2) As  $N$  increases, the behavior of these same analytic functions rapidly changes character, with the exception of the symmetric stretch/breathing motion (part i) below.

i) In the  $[N]$  sector, the breathing motion of the radial  $[N]$  mode retains this character as  $N$  increases with the symmetric radial displacements simply decreasing in amplitude.

ii) The angular mode in the  $[N]$  sector evolves from a symmetric bending character for small  $N$  to a center of mass motion for large  $N$ . This change in character occurs for fairly small  $N$ . For example, for  $N = 10$ , the motion would be viewed more appropriately as a center of mass rigid motion of the  $N(N-1)/2 = 45$  interparticle angles making identical small adjustments, rather than viewed as a symmetric bending motion.

iii) and iv) The asymmetric stretch and asymmetric bending character of the normal modes in the  $[N-1, 1]$  sector for low  $N$  evolves smoothly into radial and angular single particle excitations, i.e. particle-hole excitations. Again, this happens quickly as  $N$  increases. By  $N = 10$ , the  $10^{th}$  particle participating in the motion of the symmetry coordinate  $[\mathbf{S}_{\vec{r}'}^{[N-1, 1]}]_{\xi=9}$  or  $[\mathbf{S}_{\vec{\gamma}'}^{[N-1, 1]}]_{\xi=9}$  has a displacement that is nine times the displacements of the other particles resulting in behavior that is viewed more appropriately as a radial or angular excitation.

v) Similarly, the bending modes of the small  $N$  systems in the  $[N-2, 2]$  sector quickly and smoothly evolve into compressional or phonon behavior as  $N$  increases.

Interestingly, this change in character from small  $N$  to large  $N$  is dictated by fairly simple analytic forms that create the evolution in character for the symmetry

coordinates. Inspecting the forms of the microscopic motions of the individual particles for the different sectors:  $[N]$ ,  $[N - 1, 1]$ , and  $[N - 2, 2]$  (See Eqs. (36, 38, 39- 41)), the relevant  $N$  dependence in the  $[N]$  sector is just in a normalization factor creating a decrease in amplitude as  $N$  increases for these symmetric motions. However in the  $[N - 1, 1]$  and  $[N - 2, 2]$  sectors, the functional  $N$  dependence is more involved. Ignoring the leading common factors including a normalization factor, the  $N$  dependence is determined by an intricate balancing of Kronecker delta functions and Heaviside functions that give zero or unity depending on the value of their indices which involve integers referring to specific particles. This intricate accounting of 1's and 0's determines the motion of the  $N$  particles of this normal mode for both small  $N$  and large  $N$ . Not surprisingly, the character depends on knowing the interplay of all the individual particles one by one, whose contributions are kept track of perfectly by the Kronecker delta and Heaviside functions.

3) The behavior of the normal modes which have a mixture of the radial and angular symmetry coordinates in the  $[N]$  and  $[N - 1, 1]$  sectors was investigated for a particular Hamiltonian of current interest, that of an ensemble of identical confined fermions in the unitary regime. This behavior is seen to transition from totally radial, i.e. a pure radial symmetry coordinate to totally angular behavior, i.e. a pure angular symmetry coordinate (or vice versa) as  $N$  changes. Thus for very small  $N$ , ( $N \leq 20$  for the  $[N]$  sector and  $N \leq 10$  for the  $[N - 1, 1]$  sector) or for very large  $N$ ,  $N \gg 1$ , the normal modes adopt the character of a pure symmetry coordinate displaying either totally radial or totally angular behavior. For some intermediate values of  $N$  there is a region where the normal coordinates show significant mixing of the radial and angular symmetry coordinates making the behavior more difficult to characterize. In some cases, when the crossing is very sharp, this region is quite small, while other cases show a broader evolution of character from radial to angular or angular to radial. For large  $N$ , the normal modes evolve into purely radial or purely angular behavior in the case of identical, confined fermions in the unitary regime. This means that the analytically derived symmetry coordinates are eigenfunctions of this first order perturbation equation. When the Hamiltonian is transformed into block diagonal form by the symmetry coordinates, the off diagonal elements are negligible in these regimes.

This result has implications for the stability of collective behavior in this regime since the symmetric coordinates are eigenfunctions of an approximate underlying Hamiltonian and thus have some degree of stability unless the system is perturbed. e.g. by an increase in temperature etc.

Although the construction of the symmetry coordinates was chosen to minimize the mathematical complexity and is not a unique basis of coordinates, the symmetry coordinates clearly contain information about the dynamics of this many-body problem of identical par-

ticles. Regardless of the strategy of their construction, they are, by definition and by construction, coordinates that transform under the irreducible representations of the symmetric group of  $N$  identical objects so the Hamiltonian of this first order equation which is invariant under the  $N!$  symmetry operations of the symmetric group is transformed to block diagonal form when expressed in this basis. In this case, the blocks are small,  $2 \times 2$ , in the  $[N]$  and  $[N - 1, 1]$  sectors that have both radial and angular representations and  $1 \times 1$  blocks, i.e. diagonal for the  $[N - 2, 2]$  sector.

This Hamiltonian term in the first order perturbation equation contains beyond-mean-field effects. Thus the normal coordinates whose frequencies and mixing coefficients depend on the interparticle interactions are, in fact, beyond-mean-field *analytic* solutions to a many-body Hamiltonian through first order.

4) Except for the center of mass frequency which separates out for all values of  $N$  at twice the trap frequency, the frequencies of oscillation of the normal modes also evolve as  $N$  increases. For the case studied of fermions in the unitary regime, the radial frequencies increase in both the  $[N]$  and  $[N - 1, 1]$  sectors while the angular frequencies trend toward the trap frequency in the case of the  $[N - 1, 1]$  sector and very small values in the case of the phonon mode in the  $[N - 2, 2]$  sector. (See Figs. 5 -7) The frequency of the  $[N - 2, 2]$  modes which starts out for low  $N$  as a bending mode with a frequency near the trap frequency quickly decreases as the motion evolves into phonon compressional behavior, going to extremely small values for this low energy mode, several orders of magnitude smaller than the trap frequency. (See Fig. 7.)

5) The normal coordinates provide a basis not just for the ground state, but for the spectrum of excited states for  $L = 0$  and for higher order corrections in the perturbation expansion. I analyzed just one of the  $N - 1$  degenerate symmetry coordinates in each of the  $[N - 1, 1]$  sectors that have a frequency of  $\bar{\omega}_1$  and just one of the  $N(N - 3)/2$  degenerate symmetry coordinates in the  $[N - 2, 2]$  sector that have a frequency of  $\bar{\omega}_2$ . In these cases, the symmetry coordinate was chosen to have the highest indice(s) possible:  $\xi = N - 1$  for  $[\mathbf{S}_{\vec{r}}^{[N-1, 1]}]_{N-1}$  and  $[\mathbf{S}_{\vec{r}}^{[N-1, 1]}]_{N-1}$  and indices  $i, j$  equal to the highest values ( $i = N - 2, j = N$ ) for  $[\mathbf{S}_{\vec{r}}^{[N-2, 2]}]_{i,j}$  in order to involve all  $N$  particles in the motion. Symmetry coordinates with lower values for  $\xi$  or  $i$  and  $j$  would result in modified behavior involving fewer particles from that analyzed in Section V. This raises the question of what behavior is actually dominant in an ensemble? A definitive answer to this question is answered by obtaining the actual wave function for a particular state of  $N$  bosons or fermions with the correct permutation symmetry enforced and looking at the dominant contributions from the degenerate normal modes of the  $[N - 1, 1]$  or  $[N - 2, 2]$  sectors. Some light can be shed on this question by noting that as  $N$  increases a higher and higher percentage of the degenerate symmetry coordinates in the  $[N - 1, 1]$

and  $[N - 2, 2]$  sectors will have evolved into the “large  $N$ ” collective behavior as described above. For example, for  $N = 10$ , over 80 % of the degenerate symmetry coordinates in the  $[N - 1, 1]$  sectors have evolved into motion that is more appropriately described as single particle radial excitation or single particle angular excitation behavior rather than an antisymmetric stretching or bending motion. For  $N = 100$ , over 90% of these degenerate symmetry coordinates have evolved into “large  $N$ ” collective behavior. Similarly in the  $[N - 2, 2]$  sector, for  $N = 10$ , over 80% of the  $N(N - 3)/2$  degenerate symmetry coordinates have evolved into “large  $N$ ” collective behavior with a single dominant interparticle angle and significantly smaller responses from the remaining interparticle angles. For  $N = 100$ , the percentage is over 90% and by  $N = 1000$ , over 99% of the degenerate symmetry coordinates in this sector have “large  $N$ ” collective behavior.

**Conclusions.** This investigation into the evolution of collective behavior as a function of  $N$  suggests that this type of collective behavior defined by the normal modes of the system smoothly and quickly evolves from the well-known vibrational motions of small  $N$  systems that have been characterized as symmetric breathing and bending, asymmetric stretching and bending and the simultaneous opening and closing of interparticle angles, to the “large  $N$ ” collective behavior that is more appropriately described as breathing, center of mass, radial and angular particle-hole excitations and phonon. Thus, the analysis of behavior for these five analytic expressions for the normal mode solutions for a confined system of  $N$  identical particles yields consistent, physically intuitive behaviors that have been observed in the laboratory. The transition to “large  $N$ ” collective behavior happens at very low values of  $N$  e.g.  $N = 10$ , which is consistent with the good agreement obtained in previous few-body studies for thermodynamic quantities[41–48].

What are the dynamics that can drive one of these collective behaviors to become the dominant behavior of a system with competing behaviors, collective or not, suppressed? My analysis of the  $N$  dependence of the symmetry coordinates for a Hamiltonian that is known to support collective behavior in the form of superfluidity at ultracold temperatures in the unitary regime has revealed two phenomena that have the potential to support the creation and stabilization of collective behavior. First the mixing of radial and angular behavior in the normal modes is seen to limit to pure radial or pure angular behavior for very large  $N$  resulting in symmetry coordinates that are eigenfunctions of an approximate Hamiltonian governing the physics of the unitary regime, thus acquiring some amount of stability if unperturbed. Second, from Figs. (5)-(7), one can see that for low values of  $N$  the five different frequencies start out closer in value, but as  $N$  increases these five frequencies spread out creating large gaps between the values of these five frequencies. These gaps could provide the stability for collective be-

havior if mechanisms to prevent the transfer of energy to other modes exist (such as low temperatures) or can be constructed.

## VII. ACKNOWLEDGMENTS

I would like to thank the National Science Foundation for financial support under Grant No. PHY-1607544.

### Appendix A: The Symmetric Group and the Theory of Group Characters

A group of transformations is a set of transformations which satisfy the composition law  $ab = c$  where  $a$  and  $b$  are any two elements of the group and  $c$  also belongs to the group. A group also contains the identity element  $I$  such that  $aI = Ia = a$  and for every element in the group its inverse is also to be found in the group.

The symmetric group  $S_N$  is the group of all permutations of  $N$  objects and, as such, has  $N!$  elements. A permutation may be written as

$$\begin{pmatrix} 1 & 2 & 3 & 4 & 5 & 6 & 7 & 8 \\ 2 & 3 & 1 & 5 & 4 & 7 & 6 & 8 \end{pmatrix} \quad (\text{A1})$$

This denotes the following transformation

Object before transformation	→	is transformed to object
1	→	2
2	→	3
3	→	1
4	→	5
5	→	4
6	→	7
7	→	6
8	→	8

A cycle is a particular kind of permutation where the object labels are permuted into each other cyclically. For example the cycle  $(abc)$  means that object  $a$  is transformed into object  $b$ , object  $b$  is transformed into object  $c$  and object  $c$  is transformed into object  $a$ . The cycle  $(abc)$  is termed a 3-cycle since it cycles three objects. Like wise  $(3479)$  is a 4-cycle and  $(5)$  is a 1-cycle, the latter transforms object five into itself. All  $N!$  permutations of the group  $S_N$  may be decomposed into cycles. For example, the permutation of Eq. (A1) may be decomposed into cycles as

$$\begin{pmatrix} 1 & 2 & 3 & 4 & 5 & 6 & 7 & 8 \\ 2 & 3 & 1 & 5 & 4 & 7 & 6 & 8 \end{pmatrix} = (123)(45)(67)(8) \quad (\text{A2})$$

This consists of one 1-cycle, two 2-cycles and one 3-cycle. We can denote the cycle structure of a permutation by

the symbol  $(1^{\nu_1}, 2^{\nu_2}, 3^{\nu_3}, \dots, N^{\nu_N})$ , [36] where the notation  $j^{\nu_j}$  means a cycle of length  $j$  and  $\nu_j$  equals the number of cycles of length  $j$  in that permutation. In the case of the permutation of Eq. (A2), its cycle structure is  $(1^1, 2^2, 3^1)$ .

A matrix representation of a group is a set of nonsingular matrices, including the unit matrix, which has the same composition law as the elements of the group. The character of an element of a matrix representation of a group is the trace of the matrix. The character, as the trace of a matrix, is invariant under a similarity transformation and thus elements of equivalent representations have the same character. The set of all the distinct characters of the elements of an irreducible representation of the group uniquely specify the irreducible representation up to an equivalence transformation. The characters of irreducible representations of a group are termed *simple* characters. All elements of a group which are related by a similarity transformation are said to belong to the same class. The character of the elements of a group belonging to a particular class all have the same character. Thus there are as many distinct characters for a group as there are classes.

For the group  $S_N$  all elements with the same cycle structure belong to the same class and so all elements of a matrix representation of  $S_N$  with the same cycle structure have the same character.

A reducible matrix representation of a group may be brought to block diagonal form by a similarity transformation, where the individual blocks are irreducible matrix representations of the same group with lower dimensionality. Thus the characters,  $\chi(R)$ , of a reducible group are the sums of the characters of the irreducible matrix representations into which it can be decomposed, i.e.

$$\chi(R) = \sum_p \chi_p(R), \quad (\text{A3})$$

where  $R$  denotes the element of the group,  $p$  labels all of the irreducible blocks into which the reducible matrix representation of the group may be decomposed and  $\chi_p(R)$  is the character of the irreducible representation of the block labelled by  $p$ . Now in a particular reducible representation a given irreducible representation may be repeated along the diagonal  $a_\alpha$  times and so Eq. (A3) may be rewritten as

$$\chi(R) = \sum_\alpha a_\alpha \chi_\alpha(R). \quad (\text{A4})$$

The decomposition of  $\chi(R)$  of Eq. (A4) into simple characters  $\chi_\alpha(R)$  is unique, i.e. there is not another decomposition of the form

$$\chi(R) = \sum_\alpha b_\alpha \chi_\alpha(R), \quad (\text{A5})$$

where at least one of the  $b_\alpha$  is different from the corresponding  $a_\alpha$ . This follows from the fact that quite gen-

erally

$$a_\alpha = \frac{1}{h} \sum_R \chi_\alpha^*(R) \chi(R) \quad (\text{A6})$$

and that the simple characters satisfy the orthogonality condition

$$\sum_R \chi_\alpha^*(R) \chi_\beta(R) = h \delta_{\alpha\beta}, \quad (\text{A7})$$

where  $h$  is the number of elements in the group. For Eqs. (A5), (A6) and (A7) to be consistent we must have

$$b_\alpha = a_\alpha. \quad (\text{A8})$$

The irreducible matrix representations of  $S_N$  may be labelled by a Young diagram (= Young pattern = Young shape). A Young diagram is a set of  $N$  adjacent squares such that the row below a given row of squares is equal to or shorter in length. The set of all Young diagrams that can be formed from  $N$  boxes of all possible irreducible matrix representations of  $S_N$ .

A given Young diagram may be denoted by a partition. A partition,  $[\lambda_1, \lambda_2, \lambda_3, \dots, \lambda_N]$  is a series of  $N$  numbers  $\lambda_i$  such that  $\lambda_1 \geq \lambda_2 \geq \lambda_3 \geq \dots \geq \lambda_N$  such that  $\lambda_1 + \lambda_2 + \lambda_3 + \dots + \lambda_N = N$ . The number  $\lambda_i$  is the number of boxes in row  $i$  of the Young diagram. Thus the set of all possible partitions of length  $N$  labels all of the possible irreducible matrix representations of  $S_N$  and so the irreducible representation labels  $\alpha$  and  $\beta$  in Eqs. (A4), (A5), (A6), (A7) and (A8) above, for the group  $S_N$  may be taken to run over the set of all possible partitions.

A Young diagram can have up to  $N$  rows. For an  $N$ -row (one-column) Young diagram all of the  $\lambda_i$ s are non zero. However only one Young diagram will have  $N$  row; all of the rest will have less than  $N$  rows. Thus in all but one case the last few  $\lambda_i$ s will be zero. It is standard practice to drop the zeros and use a partition with less than  $N$  numbers. Thus the partition  $[3, 0, 0]$  labelling an irreducible representation of  $S_3$  is usually abbreviated to just  $[3]$ .

## Appendix B: Calculation of the $G$ and $FG$ matrix elements in the symmetry-coordinate basis for the $[N]$ sector.

In this Appendix we use the  $W_{\mathbf{X}'}^{[N]}$  matrices ( $\mathbf{X}' = \bar{\mathbf{r}}'$  or  $\bar{\mathbf{r}}'$ ) to calculate the  $G$  and  $FG$  matrix elements in the symmetry-coordinate basis,  $[\sigma_{[N]}^G]_{\mathbf{X}'_1, \mathbf{X}'_2}$  and  $[\sigma_{[N]}^{FG}]_{\mathbf{X}'_1, \mathbf{X}'_2}$ , using:

$$[\sigma_{[N]}^Q]_{\mathbf{X}'_1, \mathbf{X}'_2} = (W_{\mathbf{X}'_1}^{[N]})_\xi Q_{\mathbf{X}'_1 \mathbf{X}'_2} [(W_{\mathbf{X}'_2}^{[N]})_\xi]^T. \quad (\text{B1})$$

where  $Q = G$  or  $FG$  and  $\xi$  is a row label. These elements are used to obtain the mixing angles in Eq. (32), the normal mode frequencies in Eqs. (27) and (28), and the normalization coefficients in Eqs. (33) and (34).

Using Eq. (19)

$$[W_{\tilde{\mathbf{r}}'}^{[N]}]_i = \frac{1}{\sqrt{N}} [\mathbf{1}_{\tilde{\mathbf{r}}'}]_i \quad (\text{B2})$$

and Eq. (20)

$$[W_{\tilde{\boldsymbol{\gamma}}'}^{[N]}]_{ij} = \sqrt{\frac{2}{N(N-1)}} [\mathbf{1}_{\tilde{\boldsymbol{\gamma}}'}]_{ij} \quad (\text{B3})$$

with Eq.(28) in Ref. [20]

$$\mathbf{G} = \begin{pmatrix} \mathbf{I}_N & \mathbf{0} \\ \mathbf{0} & \tilde{g}' \mathbf{I}_M + \tilde{h}' \mathbf{R}^T \mathbf{R} \end{pmatrix}, \quad (\text{B4})$$

where  $G$  is an  $N(N+1)/2 \times N(N+1)/2$  matrix in the internal displacement coordinates,  $\mathbf{I}_N$  is an  $N \times N$  identity matrix,  $\mathbf{I}_M$  is an  $M \times M$  identity matrix with  $M = N(N-1)/2$ ,  $\mathbf{R}$  is an  $N \times M$  matrix such that  $R_{i,jk} = \delta_{ij} + \delta_{ik}$ , and  $\tilde{g}'$  and  $\tilde{h}'$  are defined in Ref. [20] in Eq.(29), we find:

$$\begin{aligned} [\sigma_{[N]}^G]_{\tilde{\mathbf{r}}', \tilde{\mathbf{r}}'} &= \sum_{i,j=1}^N [W_{\tilde{\mathbf{r}}'}^{[N]}]_i [\mathbf{G}_{\tilde{\mathbf{r}}', \tilde{\mathbf{r}}'}]_{ij} [(W_{\tilde{\mathbf{r}}'}^{[N]})^T]_j \\ &= \frac{1}{N} \sum_{i,j=1}^N [\mathbf{1}_{\tilde{\mathbf{r}}'}]_i \delta_{ij} [\mathbf{1}_{\tilde{\mathbf{r}}'}]_j \\ &= \frac{1}{N} \sum_i^N 1 \\ &= 1, \end{aligned} \quad (\text{B5})$$

$$\begin{aligned} [\sigma_{[N]}^G]_{\tilde{\mathbf{r}}', \tilde{\boldsymbol{\gamma}}'} &= \sum_{i=1}^N \sum_{k=2}^N \sum_{j=1}^{k-1} [W_{\tilde{\mathbf{r}}'}^{[N]}]_i [\mathbf{G}_{\tilde{\mathbf{r}}', \tilde{\boldsymbol{\gamma}}'}]_{i,jk} [(W_{\tilde{\boldsymbol{\gamma}}'}^{[N]})^T]_{jk} \\ &= 0, \end{aligned} \quad (\text{B6})$$

$$\begin{aligned} [\sigma_{[N]}^G]_{\tilde{\boldsymbol{\gamma}}', \tilde{\mathbf{r}}'} &= \sum_{j=2}^N \sum_{i=1}^{j-1} \sum_{k=1}^N [W_{\tilde{\boldsymbol{\gamma}}'}^{[N]}]_{ij} [\mathbf{G}_{\tilde{\boldsymbol{\gamma}}', \tilde{\mathbf{r}}'}]_{ij,k} [(W_{\tilde{\mathbf{r}}'}^{[N]})^T]_k \\ &= 0 \end{aligned} \quad (\text{B7})$$

and

$$\begin{aligned}
[\sigma_{[N]}^G]_{\bar{\gamma}', \bar{\gamma}'} &= \sum_{j=2}^N \sum_{i=1}^{j-1} \sum_{l=2}^N \sum_{k=1}^{l-1} [W_{\bar{\gamma}'}^{[N]}]_{ij} [\mathbf{G}_{\bar{\gamma}' \bar{\gamma}'}]_{ij, kl} [(W_{\bar{\gamma}'}^{[N]})^T]_{kl} \\
&= \frac{2}{N(N-1)} \sum_{j=2}^N \sum_{i=1}^{j-1} \sum_{l=2}^N \sum_{k=1}^{l-1} [\mathbf{1}_{\bar{\gamma}'}]_{ij} (\tilde{g}'(\delta_{ik}\delta_{jl} + \delta_{il}\delta_{jk}) + \tilde{h}'(\delta_{ik} + \delta_{il} + \delta_{jk} + \delta_{jl})) [\mathbf{1}_{\bar{\gamma}'}]_{kl} \\
&= \frac{2}{4N(N-1)} \left( \sum_{i,j,k,l=1}^N [\tilde{g}'(\delta_{ik}\delta_{jl} + \delta_{il}\delta_{jk}) + \tilde{h}'(\delta_{ik} + \delta_{il} + \delta_{jk} + \delta_{jl})] \right. \\
&\quad - \sum_{i,j,k=1}^N [\tilde{g}'(\delta_{ik}\delta_{jk} + \delta_{ik}\delta_{jk}) + \tilde{h}'(\delta_{ik} + \delta_{ik} + \delta_{jk} + \delta_{jk})] \\
&\quad - \sum_{i,k,l=1}^N [\tilde{g}'(\delta_{ik}\delta_{il} + \delta_{il}\delta_{ik}) + \tilde{h}'(\delta_{ik} + \delta_{il} + \delta_{ik} + \delta_{il})] \\
&\quad \left. + \sum_{i,k=1}^N [\tilde{g}'(\delta_{ik}\delta_{ik} + \delta_{ik}\delta_{ik}) + \tilde{h}'(\delta_{ik} + \delta_{ik} + \delta_{ik} + \delta_{ik})] \right) \\
&= \frac{1}{2N(N-1)} [(2\tilde{g}'N^2 - 4\tilde{h}'N^3) - 2(2\tilde{g}'N + 4\tilde{h}'N^2) + (2\tilde{g}'N + 4\tilde{h}'N)] \\
&= \tilde{g}' + 2\tilde{h}'(N-1).
\end{aligned}$$

Thus we obtain:

$$\sigma_{[N]}^G = \begin{pmatrix} [\sigma_{[N]}^G]_{\bar{r}', \bar{r}'} = 1 & [\sigma_{[N]}^G]_{\bar{r}', \bar{\gamma}'} = 0 \\ [\sigma_{[N]}^G]_{\bar{\gamma}', \bar{r}'} = 0 & [\sigma_{[N]}^G]_{\bar{\gamma}', \bar{\gamma}'} = (\tilde{g}' + 2(N-1)\tilde{h}') \end{pmatrix}. \quad (\text{B8})$$

where  $\sigma_{[N]}^G$  is a  $2 \times 2$  matrix representation of  $G$  for this  $[N]$  sector, i.e. in the basis of the two symmetry coordinates:  $\mathbf{S}_{\bar{r}'}^{[N]}$  and  $\mathbf{S}_{\bar{\gamma}'}^{[N]}$ .

Similarly letting  $\mathbf{Q} = \mathbf{F}\mathbf{G}$  and again using Eq.(28) in Ref. [20]:

$$\mathbf{F}\mathbf{G} = \begin{pmatrix} \tilde{a}\mathbf{I}_N + \tilde{b}\mathbf{J}_N & \tilde{e}\mathbf{R} + \tilde{f}\mathbf{J}_{NM} \\ \tilde{c}\mathbf{R}^T + \tilde{d}\mathbf{J}_{MN} & \tilde{g}\mathbf{I}_M + \tilde{h}\mathbf{R}^T\mathbf{R} + \tilde{i}\mathbf{J}_M \end{pmatrix}, \quad (\text{B9})$$

where  $\tilde{a}, \tilde{b}, \tilde{c}, \tilde{d}, \tilde{e}, \tilde{f}, \tilde{g}, \tilde{h}$ , and  $\tilde{i}$  are defined in Ref. [20]

Eq. 29, we can derive:

$$\begin{aligned}
[\sigma_{[N]}^{\mathbf{F}\mathbf{G}}]_{\bar{r}', \bar{r}'} &= \sum_{i,j=1}^N [W_{\bar{r}'}^{[N]}]_i [\mathbf{F}\mathbf{G}_{\bar{r}' \bar{r}'}]_{ij} [(W_{\bar{r}'}^{[N]})^T]_j \\
&= \frac{1}{N} \sum_{i,j=1}^N [\mathbf{1}_{\bar{r}'}]_i (\tilde{a}\delta_{ij} + \tilde{b}\mathbf{1}_{ij}) [\mathbf{1}_{\bar{r}'}]_j \\
&= \frac{1}{N} [N\tilde{a} + \tilde{b}N^2] \\
&= \tilde{a} + \tilde{b}N, \quad (\text{B10})
\end{aligned}$$

$$\begin{aligned}
[\sigma_{[N]}^{FG}]_{\bar{r}', \bar{\gamma}'} &= \sum_{i=1}^N \sum_{k=2}^N \sum_{j=1}^{k-1} [W_{\bar{r}'}^{[N]}]_i [\mathbf{F}G_{\bar{r}'\bar{\gamma}'}]_{i,j,k} [(W_{\bar{\gamma}'}^{[N]})^T]_{jk} = \frac{1}{N} \sqrt{\frac{2}{N-1}} \sum_{i=1}^N \sum_{k=2}^N \sum_{j=1}^{k-1} [\mathbf{1}_{\bar{r}'}]_i \left( \tilde{e}(\delta_{ij} + \delta_{ik}) + \tilde{f} \right) [\mathbf{1}_{\bar{\gamma}'}]_{jk} \\
&= \frac{1}{N\sqrt{2(N-1)}} \left( \sum_{i,j,k=1}^N \tilde{e}(\delta_{ij} + \delta_{ik}) + \tilde{f} - \sum_{i,j}^N \tilde{e}(\delta_{ij} + \delta_{ij}) + \tilde{f} \right) \\
&= \frac{1}{N\sqrt{2(N-1)}} (2\tilde{e}N^2 + \tilde{f}N^3 - 2\tilde{e}N - \tilde{f}N^2) = \sqrt{2(N-1)} \left( \tilde{e} + \frac{N}{2}\tilde{f} \right), \\
[\sigma_{[N]}^{FG}]_{\bar{\gamma}', \bar{r}'} &= \sum_{j=2}^N \sum_{i=1}^{j-1} \sum_{k=1}^N [W_{\bar{\gamma}'}^{[N]}]_{ij} [\mathbf{F}G_{\bar{\gamma}'\bar{r}'}]_{ij,k} [(W_{\bar{r}'}^{[N]})^T]_k = \frac{1}{N} \sqrt{\frac{2}{N-1}} \sum_{j=2}^N \sum_{i=1}^{j-1} \sum_{k=1}^N [\mathbf{1}_{\bar{\gamma}'}]_{ij} \left[ \tilde{c}(\delta_{ki} + \delta_{kj}) + \tilde{d} \right] [\mathbf{1}_{\bar{r}'}]_k \\
&= \frac{1}{N\sqrt{2(N-1)}} \left( \sum_{i,j,k=1}^N [\tilde{c}(\delta_{ki} + \delta_{kj}) + \tilde{d}] - \sum_{ik=1}^N [\tilde{c}(\delta_{ki} + \delta_{ki}) + \tilde{d}] \right) \\
&= \frac{1}{N\sqrt{2(N-1)}} (2\tilde{c}N^2 + \tilde{d}N^3 - 2\tilde{c}N - \tilde{d}N^2) = \sqrt{2(N-1)} \left( \tilde{c} + \frac{N}{2}\tilde{d} \right)
\end{aligned}$$


---

and

---

$$\begin{aligned}
[\sigma_{[N]}^{FG}]_{\bar{\gamma}', \bar{\gamma}'} &= \sum_{j=2}^N \sum_{i=1}^{j-1} \sum_{l=2}^N \sum_{k=1}^{l-1} [W_{\bar{\gamma}'}^{[N]}]_{ij} [\mathbf{F}G_{\bar{\gamma}'\bar{\gamma}'}]_{ij,kl} [(W_{\bar{\gamma}'}^{[N]})^T]_{kl} \\
&= \frac{2}{N(N-1)} \left( \sum_{j=2}^N \sum_{i=1}^{j-1} \sum_{l=2}^N \sum_{k=1}^{l-1} [\mathbf{1}_{\bar{\gamma}'}]_{ij} [\tilde{g}(\delta_{ik}\delta_{jl} + \delta_{il}\delta_{jk}) + \tilde{h}(\delta_{ik} + \delta_{il} + \delta_{jk} + \delta_{jl}) + \tilde{i}] [\mathbf{1}_{\bar{\gamma}'}]_{kl} \right) \\
&= \frac{1}{2N(N-1)} \left( \sum_{i,j,k,l=1}^N [\tilde{g}(\delta_{ik}\delta_{jl} + \delta_{il}\delta_{jk}) + \tilde{h}(\delta_{ik} + \delta_{il} + \delta_{jk} + \delta_{jl}) + \tilde{i}] \right. \\
&\quad - \sum_{i,j,k=1}^N (\tilde{g}(\delta_{ik}\delta_{jk} + \delta_{ik}\delta_{jk}) + \tilde{h}(\delta_{ik} + \delta_{ik} + \delta_{jk} + \delta_{jk}) + \tilde{i}) \\
&\quad - \sum_{i,k,l=1}^N (\tilde{g}(\delta_{ik}\delta_{il} + \delta_{il}\delta_{ik}) + \tilde{h}(\delta_{ik} + \delta_{il} + \delta_{ik} + \delta_{il}) + \tilde{i}) \\
&\quad \left. + \sum_{i,k=1}^N (\tilde{g}(\delta_{ik}\delta_{ik} + \delta_{ik}\delta_{ik}) + \tilde{h}(\delta_{ik} + \delta_{ik} + \delta_{ik} + \delta_{ik}) + \tilde{i}) \right) \\
&= \frac{1}{2N(N-1)} (2N(N-1)\tilde{g} + 4N(N^2 - 2N + 1)\tilde{h} + N^2(N^2 - 2N + 1)\tilde{i}) \\
&= \tilde{g} + 2(N-1)\tilde{h} + \frac{N(N-1)}{2} \tilde{i}.
\end{aligned}$$


---

Thus we obtain the  $2 \times 2$  matrix representation of  $FG$  in the symmetry basis of the  $[N]$  sector.

---

$$\sigma_{[N]}^{FG} = \begin{pmatrix} [\sigma_{[N]}^{FG}]_{\bar{r}', \bar{r}'} = (\tilde{a} + \tilde{b}N) & [\sigma_{[N]}^{FG}]_{\bar{r}', \bar{\gamma}'} = \sqrt{2(N-1)} \left( \tilde{e} + \frac{N}{2}\tilde{f} \right) \\ [\sigma_{[N]}^{FG}]_{\bar{\gamma}', \bar{r}'} = \sqrt{2(N-1)} \left( \tilde{c} + \frac{N}{2}\tilde{d} \right) & [\sigma_{[N]}^{FG}]_{\bar{\gamma}', \bar{\gamma}'} = \left( \tilde{g} + 2(N-1)\tilde{h} + \frac{N(N-1)}{2} \tilde{i} \right) \end{pmatrix}. \quad (\text{B11})$$

- 
- [1] N. Zagar, J. Boyd, A. Kasaara, J. Tribbia, E. Kallen, H. Tanaka, and J.-i Yano, *Bull. Am. Meteor. Soc.* **97** (2016).
- [2] S.C. Webb, *Geophys.J. Int.* **174**, 542(2008).
- [3] B.V. Sanchez, *J. Marine Geodesy* **31**, 181(2008).
- [4] D.L. Rousseau, R.T. Bauman, S.P.S. Porto, J. Ramam Spect., **10**, 253(1981).
- [5] J. Lee, K.T. Crampton, N. Tallarida, and V.A. Apkarian, *Nature* **568**, 78(2019).
- [6] L. Fortunato, *EPJ Web of Conferences* **178**, 02017 (2018).
- [7] E.C. Dykeman and O.F. Sankey, *J. Phys.:Condens. Matter* **22**, 423202(2010).
- [8] M.J. Clement, *App J.* **249**, 746(1981).
- [9] M. Coughlin and J. Harms, arXiv:1406.1147v1 [gr-qc] (2014).
- [10] K. D. Kokkolas, *Class. Quantum Grav.* **8**, 2217 (1991).
- [11] R.M. Stratt, *Acc. Chem. Res.* **28**, 201(1995).
- [12] C.R. McDonald, G. Orlando, J.W. Abraham, D. Hochstuhl, M. Bonitz, and T. Brabee, *Phys. Rev. Lett.* **111**, 256801 (2013); F. Dalfove, S. Giorgini, L.P. Pitaevskii, and S. Stringari, *Rev. Mod. Phys.* **71**, 463(1999); D. Jaksch, C. Bruder, J.I. Cirac, C.W. Gardiner, and P. Zoller, *Phys. Rev. Lett.* **81**, 3108(1998); H. Dong, W. Zhang, L. Zhou and Y. Ma, *Sci. Rep.* **5**, 15848; doi: 10.1038/srep15848(2015).
- [13] H.C. Nagerl, C. Roos, H. Rohde, D. Leibfried, J. Eschner, F. Schmidt-Kaler and R. Blatt, *Fortschr. Phys.* **48**, 623 (2000).
- [14] Anderson, P.W., *Science* **177**, 393(1972).
- [15] P.W. Anderson, *Nature* **437**, 625 (2005).
- [16] M. Guidry and Y. Sun, *Frontiers of Physics*, **10**, 1 (2015).
- [17] R.B. Laughlin and D. Pines, *PNAS* **97**, 28 (2000).
- [18] J. Zaanen, *Science* **319**, 1205 (2008).
- [19] D.K. Watson, "Universal thermodynamics of a trapped Fermi gas in the superfluid regime: the role of the Pauli principle", accepted *J. Phys. B.*, <https://doi.org/10.1088/1361-6455/ab3c11>.
- [20] M. Dunn, D.K. Watson, and J.G. Loeser, *Ann. Phys. (NY)*, **321**, 1939 (2006).
- [21] W.B. Laing, M. Dunn, and D.K. Watson, *J. of Math. Phys.* **50**, 062105 (2009).
- [22] B.A. McKinney, M. Dunn, D.K. Watson, and J.G. Loeser, *Ann. Phys.* **310**, 56 (2003).
- [23] W.B. Laing, D.W. Kelle, M. Dunn, and D.K. Watson, *J Phys A* **42**, 205307 (2009).
- [24] M. Dunn, W.B. Laing, D. Toth, and D.K. Watson, *Phys. Rev A* **80**, 062108 (2009).
- [25] D.K. Watson and M. Dunn, *Phys. Rev. Lett.* **105**, 020402 (2010).
- [26] D.K. Watson and M. Dunn, *J. Phys. B* **45**, 095002 (2012).
- [27] W.B. Laing, M. Dunn, and D.K. Watson, EPAPS Document Number E-JMAPAQ-50-031904.
- [28] B.A. McKinney, M. Dunn, D.K. Watson, *Phys. Rev. A* **69**, 053611 (2004).
- [29] W.B. Laing, M. Dunn, and D.K. Watson, *Phys. Rev. A* **74**, 063605 (2006).
- [30] D.K. Watson, *Phys. Rev. A* **92**, 013628 (2015).
- [31] D.K. Watson, *Phys. Rev. A* **93**, 023622 (2016).
- [32] D.K. Watson, *Phys. Rev. A* **96**, 033601(2017).
- [33] J. Avery, D.Z. Goodson, D.R. Herschbach, *Theor. Chim. Acta* **81**, 1 (1991).
- [34] A. Chatterjee, *J. Phys. A: Math. Gen.* **18**, 735 (1985).
- [35] E.B. Wilson, Jr., J.C. Decius, P.C. Cross, *Molecular vibrations: The theory of infrared and raman vibrational spectra*. McGraw-Hill, New York, 1955.
- [36] M. Hamermesh, *Group theory and its application to physical problems*. Addison-Wesley, Reading, MA, 1962.
- [37] J.G. Loeser, *J. Chem. Phys.* **86**, 5635 (1987).
- [38] See for example Ref. [35], Appendix XII, p. 347.
- [39] F.R. Gantmacher, *The theory of matrices, Vol. 1*. Chelsea, New York, 1959.
- [40] See for example Ref. [36], p. 100.
- [41] S.K. Adhikari, *Phys. Rev. A* **79**, 023611(2009).
- [42] X.-J. Liu, H. Hu, and P.D. Drummond, *Phys. Rev. Lett.* **102**, 160401 (2009).
- [43] X.-J. Liu, H. Hu, and P.D. Drummond, *Phys. Rev. A* **82**, 023619 (2010).
- [44] X.-J. Liu, H. Hu, and P.D. Drummond, *Phys. Rev. B* **82**, 054524 (2010).
- [45] T. Grining, M. Tomza, M. Lesiuk, M. Przybytek, M. Mursial, R. Moszynski, M. Lewenstein, and P. Massignan, *PRA* **92**, 061601 (2015).
- [46] D. Blume, *Physics* **3**, 74 (2010).
- [47] D. Blume, *Rep. Prog. Phys.* **75**, 046401 (2012).
- [48] J. Levinsen, P. Massignan, S. Endo, and M.M. Parish, *J. Phys. B* **50**, 072001 (2017).